



HAL
open science

Anatomy and evolution of a migmatite-cored extensional metamorphic dome and interaction with syn-kinematic intrusions, the Mykonos-Delos-Rheneia MCC

Laurent Jolivet, Violaine Sautter, Isabelle Moretti, Tommy Vettor, Zozi Papadopoulou, Romain Augier, Yoann Denèle, Laurent Arbaret

► To cite this version:

Laurent Jolivet, Violaine Sautter, Isabelle Moretti, Tommy Vettor, Zozi Papadopoulou, et al.. Anatomy and evolution of a migmatite-cored extensional metamorphic dome and interaction with syn-kinematic intrusions, the Mykonos-Delos-Rheneia MCC. *Journal of Geodynamics*, 2021, pp.101824. 10.1016/j.jog.2021.101824 . insu-03141088v2

HAL Id: insu-03141088

<https://insu.hal.science/insu-03141088v2>

Submitted on 3 Mar 2021

HAL is a multi-disciplinary open access archive for the deposit and dissemination of scientific research documents, whether they are published or not. The documents may come from teaching and research institutions in France or abroad, or from public or private research centers.

L'archive ouverte pluridisciplinaire **HAL**, est destinée au dépôt et à la diffusion de documents scientifiques de niveau recherche, publiés ou non, émanant des établissements d'enseignement et de recherche français ou étrangers, des laboratoires publics ou privés.



Distributed under a Creative Commons Attribution - NoDerivatives 4.0 International License



Anatomy and evolution of a migmatite-cored extensional metamorphic dome and interaction with syn-kinematic intrusions, the Mykonos-Delos-Rheneia MCC

Laurent Jolivet^{a,*}, Violaine Sautter^b, Isabelle Moretti^a, Tommy Vettor^b, Zozi Papadopoulou^c, Romain Augier^{d,e,f}, Yoann Denèle^g, Laurent Arbaret^{d,e,f}

^a ISTeP, Sorbonne Université, 4 Place Jussieu, 75252, Paris Cedex 05, France

^b Muséum National d'Histoire Naturelle, IMPMC, Site Buffon, Bat. 52, Rue Buffon, Paris, France

^c Ephorate of Antiquities of the Cyclades, Athens, Greece

^d Université d'Orléans, ISTO, UMR 7327, 45071, Orléans, France

^e CNRS/INSU, ISTO, UMR 7327, 45071, Orléans, France

^f BRGM, ISTO, UMR 7327, BP 36009, 45060, Orléans, France

^g Géosciences Environnement Toulouse, Université De Toulouse 3, Université Paul Sabatier, CNRS, IRD, Toulouse, France

ARTICLE INFO

Keywords:

Metamorphic core complex
Shear zone
Detachment
Migmatite
syn-Kinematic intrusion
A-type domes
Post-orogenic extension
Cyclades
Delos
Rheneia
Mykonos

ABSTRACT

Post-orogenic extension in back-arc regions is classically associated with metamorphic core complexes (MCCs) cored with exhumed metamorphic rocks and granitic intrusions interacting with low-angle detachments. When additional heat is provided by the advected asthenosphere below the extending region, for instance above slab tears, high-temperature migmatite-cored metamorphic domes and composite intrusions are emplaced whose geometry and kinematics of emplacement are controlled by regional extension and by detachments. The Cyclades Archipelago (Aegean Sea) hosts several such Miocene high-temperature MMCs intruded by Miocene granitoids, offering windows open on the interactions of intrusions with the Livada and Mykonos detachments, two branches of the North Cycladic Detachment System. Deformation associated with North Cycladic Detachment System has been described detailed on Mykonos based on a structural study of the deformation of the Mykonos pluton, but the high-temperature gneiss core of the MCC and the root zone of the intrusion have received little attention. Based on field surveys of the neighboring islands of Rheneia and Delos, we propose in this paper a new geological map and show that the locally migmatitic core of the MCC that extends from Rheneia to the Apollonia peninsula on Mykonos, is topped by a 500 m-thick low-angle shear zone, the Rheneia Shear Zone, coeval with the intrusion of a series of granitoids evolving from granodiorite to monzogranite. The Rheneia Shear Zone shows progressive flattening and shearing, with a constrictional component, during the intrusion of numerous fine-grained felsic dykes at various stages that are totally transposed to become parallel to the main regional foliation. The migmatitic core and the intrusion are intensely stretched with an E–W trending lineation and folds with axes parallel to the lineation. Structural compatibility between the migmatites and the intrusion show that the rheological parameters were not much different at the time of intrusion. The same deformation continued during cooling of the dome while new batches of granitic material intruded the colder gneiss. The granites show syn-kinematic stretching at the magmatic stage and after cooling, leading to full homoaxiality between the magmatic fabric and the mylonites below the Livada and Mykonos Detachment. From the stage of lower crustal partial melting and subsequent intrusion to mylonitization and formation of the brittle Mykonos detachment, deposition of the supra-detachment Miocene sediments and the late intrusion of baryte-iron dykes, the same kinematics is observed until a change in the stress regime some 9 Ma ago. The Mykonos-Delos-Rheneia MCC illustrates the continuous interactions between a detachment system and a growing pluton and how a discrete magmatic event can be influenced by long-term tectonics.

* Corresponding author.

E-mail address: laurent.jolivet@sorbonne-universite.fr (L. Jolivet).

<https://doi.org/10.1016/j.jog.2021.101824>

Received 24 July 2020; Received in revised form 28 January 2021; Accepted 1 February 2021

Available online 10 February 2021

0264-3707/© 2021 The Author(s). Published by Elsevier Ltd. This is an open access article under the CC BY-NC-ND license

(<http://creativecommons.org/licenses/by-nc-nd/4.0/>).

1. Introduction

The interrelations between magma emplacement and crustal deformation are governed by complex processes because of the overall large viscosity difference between upper crustal rocks and magmas. Two types of behavior are described: “active emplacement” when the magma production rate is larger than opening of voids by tectonic processes, whereas “passive” emplacement represents the opposite situation (Hutton, 1988). In this context, the fertility of magma sources would be the main driving parameter, especially when considering that the rate of magma ascent is often much higher than most tectonic processes (Paterson and Tobisch, 1992). de Saint Blanquat et al. (2011), based on a review of a large number of natural situations reached a similar conclusion whatever the scale of the pluton, pluton emplacement in the upper crust is much shorter in duration (several hundred thousand years or a few million years for the largest plutons) and occurs at much faster rates than tectonic deformation. This can explain why some plutons

emplaced during the course of an active tectonic deformation can share many characteristics of post-kinematic intrusions (de Saint-Blanquat et al., 2001).

The situation may however prove different in the case of plutons forming and then emplacing within metamorphic core complexes (MCCs). Syn-kinematic plutons have been described in different contexts, along strike-slip shear zones such as the South Armorican Shear Zone (Berthé et al., 1979; Augier et al., 2015a), or along extensional shear zones with the examples of the Basin and Range (Holm, 1995), Southeast China (Charles et al., 2011; Lin et al., 2013; Ji et al., 2018), the Variscan belt (Gapais et al., 1993; Augier et al., 2015a, 2015b), the Aegean MCCs (Faure et al., 1991; Lee and Lister, 1992; Rabillard et al., 2017) or the Paleozoic post-orogenic extension context of Calabria (Caggianelli et al., 2000). Extension is a context where space is created continuously and the plutons and their host rocks are largely exhumed so that the interactions between the activity of extensional shear zones and the coeval intrusions can be observed and described (Hutton et al.,

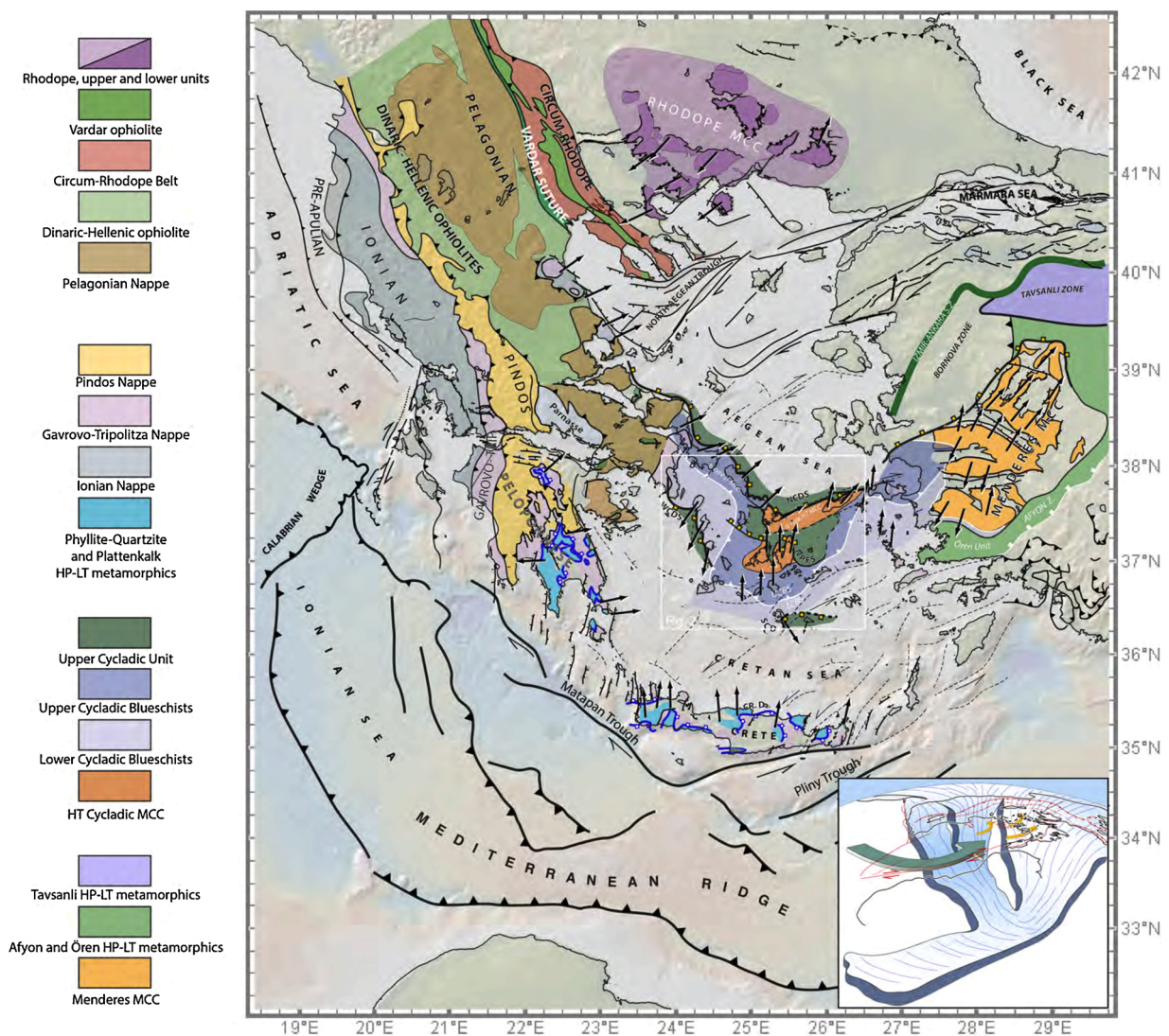


Fig. 1. Tectonic map of the Aegean region showing the main exhumed metamorphic complexes and the situation of the Cyclades. CR. D.: Cretan Detachment, NCDS: North Cycladic Detachment System, NPPS: Naxos-Paros Fault System, WCDS: West Cycladic Detachment System; SCD: South Cycladic Detachment System. The distribution of the different units in the Cycladic Blueschists is after Grasmann et al. (2017) and Roche et al. (2019). Arrows are representative kinematic indicators (lineations and sense of shear) in the various metamorphic core complexes (Gautier et al., 1993; Gautier and Brun, 1994b; Hetzel et al., 1995a; Hetzel et al., 1995b; Jolivet et al., 1996; Trotet et al., 2001a; 2001b; Grasmann and Petrakakis, 2007; Tschegg and Grasmann, 2009; Jolivet et al., 2010; Iglseider et al., 2011; Grasmann et al., 2012; Rice et al., 2012; Augier et al., 2015a; Beaudoin et al., 2015; Laurent et al., 2015; Rabillard et al., 2015; Ducoux et al., 2016; Roche et al., 2016; Grasmann et al., 2017; Rabillard et al., 2017; Roche et al., 2018; Schneider et al., 2018; Roche et al., 2019). Inset: 3D diagram showing the geometry of the slab after the tomographic model of Biryol et al. (2011).

1990; Rabillard et al., 2017). Post-orogenic extension after a phase of crustal thickening, and more specifically when it occurs in a back-arc environment where the hot asthenosphere is advected upward below the thick crust, is a favorable context to produce granitoids interacting with detachments. The Aegean Sea or the Northern Tyrrhenian Sea

provide several examples of plutons emplaced in the core of MCCs below low-angle detachments during the Miocene (Faure and Bonneau, 1988; Faure et al., 1991; Lee and Lister, 1992). Recent studies have shown a common scheme in all these plutons and their associated detachments (Beaudoin et al., 2015; Laurent et al., 2015; Rabillard et al., 2015;

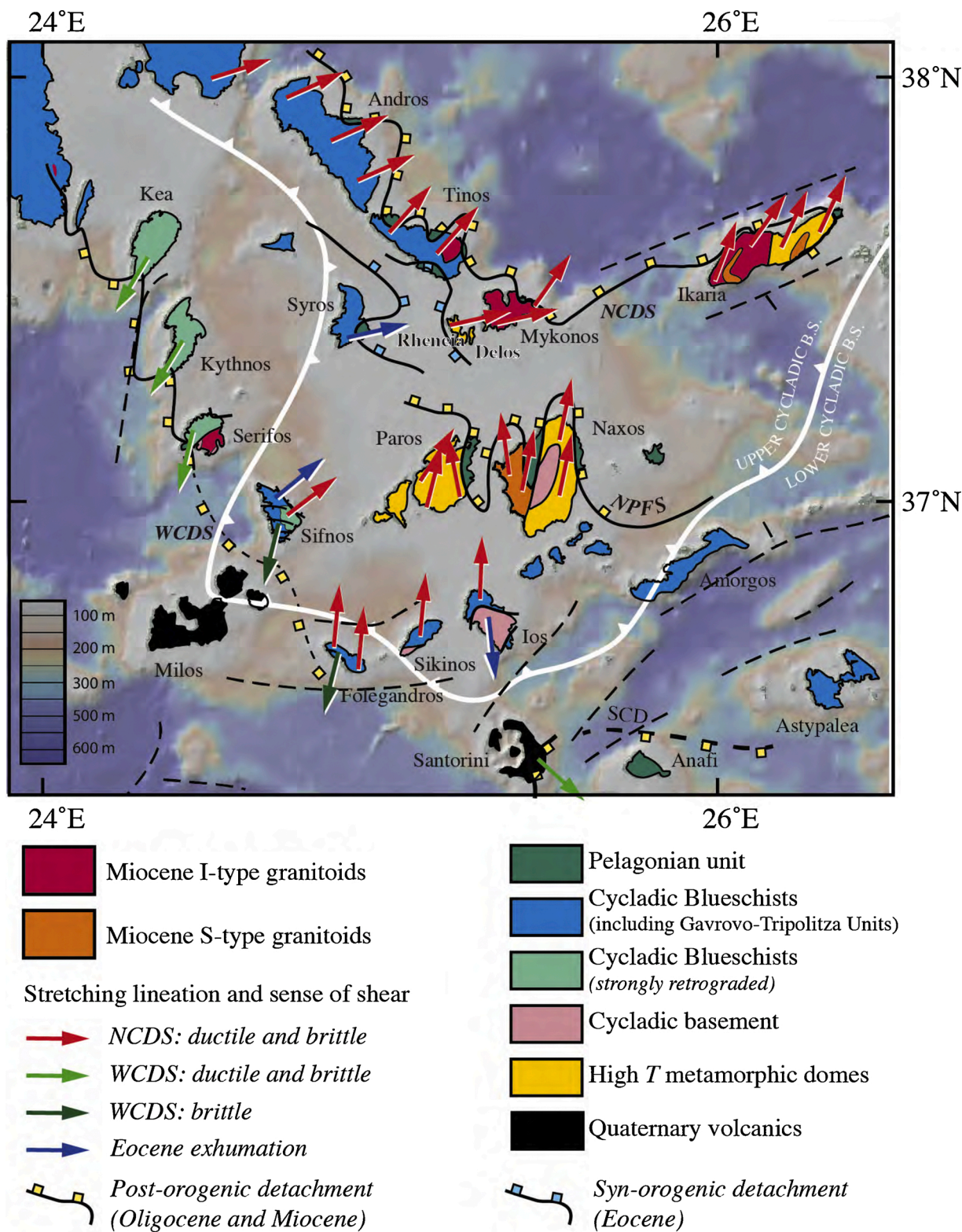


Fig. 2. Tectonic map of the Cyclades showing the main metamorphic core complexes, the high-temperature gneiss domes and associated intrusions, together with the main extensional post-orogenic lineation and sense of shear (see Fig. 1 for reference). NCDS: North Cycladic Detachment System; WCDS: West Cycladic Detachment System; SCD: South Cycladic Detachment System.

Ducoux et al., 2016; Bessière et al., 2017; Rabillard et al., 2017). The Aegean granitoid plutons were emplaced during a rather short period between 16 and 8 Ma coeval with the fast rotation of the Hellenides and formation of a first-order tear in the subducting slab (Fig. 1 inset, de Boorder et al., 1998; Biryol et al., 2011; Jolivet et al., 2015). The plutons were exhumed below two main sets of detachments, the North Cycladic Detachment System (NCDS) and the West Cycladic Detachment System (WCDS) and several of them intruded the core of MCCs made of high grade migmatitic gneiss below the NCDS (Ikaria, Mykonos-Delos-Rheneia and Naxos-Paros) while other intruded higher in the crust (e.g. Tinos, Serifos or Lavrio).

Oligo-Miocene extension in the Cyclades (Fig. 1, Fig. 2) follows an episode of continental subduction and crustal thickening in HP-LT conditions recorded in the Cycladic Blueschists Unit (CBU) during the Eocene (Altherr et al., 1982; Wijbrans and McDougall, 1988; Shaked et al., 2000; Trotet et al., 2001a; 2001b; Jolivet et al., 2004a, 2004b; Ring et al., 2007; Brun and Faccenna, 2008; Jolivet and Brun, 2010; Ring et al., 2010, 2011; Laurent et al., 2016, 2017). The heterogeneity of the crust acquired during this early stage played an important role in localizing the main extensional structures, especially the NCDS (Le Pourhiet et al., 2004; Huet et al., 2011; Augier et al., 2015a, 2015b; Labrousse et al., 2016). Compared to the underlying CBU, the Upper Cycladic Unit (UCU), shows a contrasted lithologies. It is either made of an ophiolite nappe with its basal metamorphic sole, like on Tinos Island (Katzir et al., 1996; Lamont et al., 2020) or orthogneiss or other continental basement units like on Syros (Maluski et al., 1987; Keiter et al., 2004; Soukis and Stöckli, 2013) or Anafi Islands (Reinecke et al., 1982; Martha et al., 2016). Both the inverted mechanical stratigraphy due to the overthrusting of an ophiolite nappe on top of the weaker CBU and the presence of other nappe contacts were shown to favor strain localization and formation of MCCs (Labrousse et al., 2016). The intrusion of granitoids during the Miocene within these MCC induced a migration of the detachments upward and in the direction of shearing (Rabillard et al., 2017). The NCDS and the WCDS are thus made of a succession in time and space of up to three detachments (Jolivet et al., 2010; Rabillard et al., 2017). The lower detachments are mostly active in the ductile regime and they are locally inactivated when the granitic pluton intrudes them, while the uppermost one is only brittle and controls the deposition of a supra-detachment basin (Menant et al., 2013; Rabillard et al., 2017).

The Aegean granitoids were emplaced within a short period between ~16 and 8 Ma V-(Skarpelis et al., 1992; Altherr and Siebel, 2002; Brichau et al., 2007, 2008; Liati et al., 2009; Bolhar et al., 2010). They show distinct geochemical features indicating either a mantle or crustal origin, which has been debated (Altherr and Siebel, 2002; Pe-Piper et al., 2002; Pe-Piper and Piper, 2006; Stouraiti et al., 2010; Bolhar et al., 2012). The older plutons, such as the Karkinagrion and Xylosyrtis leucogranitic plutons of Ikaria display a dominating crustal contribution and they are associated with migmatite domes, while the younger ones, such as the Tinos granodiorite have a larger mantle component. However, all plutons show a significant component of crustal melting. Granitoid bodies intrude the migmatitic core of the MCCs and then interact with the detachments (Bessière et al., 2017) during a period bracketed between 18 and 11 Ma (Ring et al., 2018). In the case of Naxos, the intrusion of the granodiorite occurred when the external part of the dome had already cooled down as shown by the occurrence of a contact metamorphism envelope in the dome at the sharp contact with the pluton (Buick and Holland, 1989; Urai et al., 1990), while on Ikaria (Beaudoin et al., 2015; Laurent et al., 2015) and Mykonos the dome was still hot and viscous as shown below. On Mykonos, most recent tectonic studies concentrated on the granitoids and their deformation below the NCDS (Faure and Bonneau, 1988; Lee and Lister, 1992; Brichau et al., 2008; Lecomte et al., 2010; Denèle et al., 2011; Menant et al., 2013). Very few studies (Lucas, 1999; Pe-Piper et al., 2002; Denèle et al., 2011) were so far dedicated to field observations in the migmatitic core on Mykonos and its extension in Delos and Rheneia because these latter

islands are not normally accessible to geological survey as they are within a perimeter reserved for archeological studies. Yet, only a small part of the migmatitic core of the MCC crops out on Mykonos where field work has been concentrated up to now. The opportunity to make a new geological map including new data from these two islands was thus an important opening.

This paper presents the results of our investigations in the field on Delos and Rheneia and their integration in the framework of the Mykonos-Delos-Rheneia (MDR) MCC, focusing on the geometry and deformation within the migmatitic core of the MCC and interactions with the main pluton. The MDR MCC completes the observations made on Ikaria where the migmatitic dome crops out only in a limited perimeter and on Naxos where the deep interactions with the hot dome are not displayed. This example shows the detailed interactions at depth between the migmatitic dome and the rising pluton, observations that cannot be easily made in the other Aegean plutons. Based on these new field observations, we propose a conceptual model of the emplacement of a pluton within a viscous migmatitic dome actively deforming and its evolution during cooling and interaction with the detachments.

2. Geological setting

The Cyclades archipelago forms a wide submarine plateau in the center of the Aegean Sea (Fig. 1) where a series of islands shows the apex of several MCC formed during the Oligocene and Miocene (Fig. 2). Extension is a consequence of slab retreat and coeval collapse of the Hellenides-Taurides mountain belt formed earlier during the Eocene by subduction and collision of a small partly oceanic basin, the Pindos Basin, and its southern margin belonging to Apulia with the southern margin of Eurasia (Le Pichon and Angelier, 1979, 1981b, a; Jolivet and Brun, 2010), to the southwest of the Vardar Ocean suture zone (Dercourt et al., 1986; Ricou et al., 1998; Schmid et al., 2008; Tremblay et al., 2015; Menant et al., 2016). The Cycladic Blueschists (Blake et al., 1984), mostly formed during this Eocene episode, were exhumed progressively. First exhumation took place during the syn-orogenic stage with an excellent preservation of blueschists-facies and eclogite-facies parageneses on Syros (Bröcker and Enders, 1999; Keiter et al., 2004; Schumacher et al., 2008; Philippon et al., 2011; Laurent et al., 2016) and Sifnos (Avigad et al., 1992; Lister and Raouzaïos, 1996; Groppo et al., 2009; Aravadinou et al., 2015; Roche et al., 2016). Then, exhumation was completed during the Late Oligocene and Miocene during the post-orogenic stage in the back-arc region of the retreating Hellenic subduction (Jolivet et al., 1994a, b; Trotet et al., 2001a; Vanderhaeghe, 2009; Jolivet and Brun, 2010; Grasemann et al., 2012). In the latter case, the HP-LT parageneses were more or less intensely overprinted in HT-LP conditions, locally reaching those of partial melting as in Naxos (Jansen, 1977; Buick and Holland, 1989; Urai et al., 1990; Keay et al., 2001; Vanderhaeghe, 2004; Duchêne et al., 2006), Paros (Papanikolaou, 1979; Bargnesi et al., 2013), Ikaria (Beaudoin et al., 2015) and Mykonos-Delos-Rheneia (Faure and Bonneau, 1988; Lucas, 1999; Denèle et al., 2011). Intermediate conditions and two-staged exhumation P - T paths are displayed in MCC that evolved progressively between the syn-orogenic and the post-orogenic stages (Tinos, Andros) (Jolivet and Brun, 2010). The late exhumation of these domes, partly coeval with emplacement of intrusions, has been dated with thermochronology, showing the progressive exhumation below the low-angle detachments (Brichau et al., 2006, 2007; 2008; Soukis and Stöckli, 2013).

Oligo-Miocene extension was distributed across the archipelago between two main detachments. The NCDS (Jolivet et al., 2010) dips mostly toward the north or the northeast. It can be followed from Evia, Andros, Tinos, Mykonos, Ikaria to Samos and extends within the Simav Detachments bounding the Menderes MCC to the north (Jolivet et al., 2013). The kinematics along the NCDS is top-to-the N/NE as observed on Mykonos. Top-to-the north kinematics is also observed on the Naxos-Paros Detachment (Urai et al., 1990; Buick, 1991; Gautier et al., 1993; Gautier and Brun, 1994b, a; Jolivet et al., 1994a, 1994b; Gautier

et al., 1999; Bargnesi et al., 2013; Bessière et al., 2017) and in more southern islands such as Ios (Huet et al., 2009) and Sikinos (Augier et al., 2015a, 2015b; Poulaki et al., 2019). The WCDS (Grasemann and Petrakakis, 2007; Iglseider et al., 2011; Grasemann et al., 2012) and its extension within the South Aegean Detachment (Grasemann et al., 2017; Grasemann et al., 2017; Schneider et al., 2018) dips toward the south or southwest with an opposite top-to-the-S/SW kinematics. Ring et al. (2011) reported the presence of a low-angle detachment with top-SW kinematic indicators on Sifnos, which they attributed to the South Cyclades Detachment. Roche et al. (2016) then showed that the same low-angle fault is in fact associated with top-NE kinematic that developed under greenschists-facies conditions. On Sifnos, only some late SW-dipping normal faults could be associated with the South Cycladic Detachment. Similar observations can be made on Folegandros (Augier et al., 2015a, 2015b). On Ios, top-S kinematic indicators in the southern half of the island have been diversely interpreted. Lister et al. (1984) used these to document the kinematics of the detachment observed further north of Naxos, which proved later to be associated with a top-N kinematics. Vandenberg and Lister (1996) described these kinematic indicators in more details. Huet et al. (2009) after a detailed mapping of kinematic indicators over the whole island have interpreted top-south criteria as either related to the pre-extension HP-LT thrust-related deformation for those associated with blueschists facies mineral phases or to conjugate to the top-N ones for the later ones for the later ones that developed under greenschist-facies condition, giving a component of co-axial strain during the Neogene extension. The northern part of the island instead shows only top-N kinematic indicators along discrete shear zones related to the Paros-Naxos detachment system. More recently, Mizera and Behrmann (2015) interpreted these same top-S kinematic indicators as related to a distinct top-south shear zone. This issue is still debated. Nonetheless, the South Cycladic Detachment and its extension in the West Cycladic Detachment, as described in Grasemann et al. (2012) and Schneider et al. (2018) extends from Lavrion, Kea, Kythnos all the way to Serifos and Santorini. The South Cycladic Detachment (SCD) has indeed been described on Santorini with a top-to-the south kinematics (Schneider et al., 2018).

Two types of MCC are recognized. « Cold » b-type MCC preserve rather well the HP-LT parageneses and they are elongated perpendicular to the main direction of stretching (e.g. Andros, Tinos) while “hot” a-type MCC, cored with HT-gneiss and migmatites, are elongated parallel to the main stretching direction (e.g. Ikaria, Naxos, Mykonos-Delos-Rheneia) (Jolivet et al., 2004a, 2004b). The hot MCCs and associated intrusions developed above a first-order tear in the Hellenic slab formed between 15 and 8 Ma (Jolivet et al., 2015), coeval with the fast clockwise rotation of the Hellenides (van Hinsbergen et al., 2005).

The core of Cycladic HT-domes of Ikaria, Mykonos-Delos-Rheneia and Naxos-Paros is characterized by micaschists and gneiss, partly migmatitic (Andriessen et al., 1987; Urai et al., 1990; Faure et al., 1991; Gautier et al., 1993; Keay et al., 2001; Duchêne et al., 2006; Beaudoin et al., 2015; Lamont et al., 2018; Vanderhaeghe et al., 2018) and are sometimes correlated with the continental basement of the Cycladic Blueschists (Jolivet et al., 2004a, 2004b; Roche et al., 2019). This basement can also be observed in the lower units of Ios and Sykinos islands where no evidence of HT-LP metamorphism is observed (Vandenberg and Lister, 1996; Augier et al., 2015a, 2015b). If a clear difference can be made on Naxos between the basement (migmatitic core) and the overlying marble cover or probably early Mesozoic depositional age, it is not so clear on Mykonos or Delos and Rheneia because most lithologies are pelitic. The presence of thick marble layers in this region is indicative of a Mesozoic depositional age but when these marbles are absent, the attribution is difficult. On Ios and Sikinos, the basement unit do not show any HT-LP metamorphism and a clear difference can be made with the overlying Cycladic Blueschists. We thus consider that the true basement can be found in the migmatitic core of Naxos and the lower units of Ios and Sikinos. Other HT units can originally belong either to the basement or to some more recent mostly pelitic

stratigraphic sequence. The age of the migmatitization is not always known with precision but recent studies in Naxos (Ring et al., 2018) and Ikaria (Beaudoin et al., 2015) show that the main episode of partial melting is early to middle Miocene in age (between 16 and 13 Ma). In this study we consider that the migmatites observed on Delos and Rheneia all date back to the same period of the Miocene as structural correlations with granitic dikes and pluton show that migmatites and granites recorded the same deformation history, that occurred during the period of granitic intrusions (see below).

The Mykonos-Delos-Rheneia MCC (Fig. 3) was one of the first described in the Aegean region (Faure and Bonneau, 1988; Faure et al., 1991; Lee and Lister, 1992). The emplacement of the Mykonos granitoids below an extensional detachment was recognized and the first-order geometry of the migmatitic dome described. Later studies showed that the core of the dome and the roots of the intrusions are located on Delos and Rheneia with rather steep magmatic and tectonic foliations contrasting with the low-angle mylonites developed below the detachment (Lucas, 1999; Denèle et al., 2011). The co-magmatic deformation within the Delos pluton and the distribution of different magmatic facies all indicate a main, locally strong E-W elongation (Lucas, 1999; Pe-Piper et al., 2002; Denèle et al., 2011). The Mykonos-Delos intrusion is a laccolith dipping shallowly toward the east on Mykonos and rooting on Delos and Rheneia in a zone of steeper foliation (Denèle et al., 2011). On Mykonos, most of the intrusion is affected by two low-angle branches of the NCDS, mapped in detail by Menant et al. (2013). The extensional activity of the detachments and the exhumation of the intrusion are documented by radiochronology and low-T thermochronology (Brichau et al., 2008) and by the detailed interactions between the pluton, the different branches of the detachments and the late mineralization (Menant et al., 2013). The lower Livada Detachment is a ductile shear zone affecting the intrusive contact of the pluton within the UCU essentially made of greenschists-facies metabasites (Jolivet et al., 2010; Lecomte et al., 2010). It is associated with a thick shear zone deforming most of the intrusion on the island. A large-scale gradient is observed from co-magmatic and late-magmatic deformation in the west toward mylonites and ultra-mylonites in the east in the vicinity of the detachment. The E-W to ENE-WSW direction of stretching and the top-to-the east sense of shear are consistent over the whole island. Conversely, the upper Mykonos Detachment is a purely brittle low-angle fault carrying a late Miocene supra-detachment basin filled with coarse clastic sediments including conglomerates, sandstones and minor shales with clear evidence of syn-extension deposition (Avigad et al., 1998; Sanchez-Gomez et al., 2002; Menant et al., 2013). Observations of the detachment plane and syn-sedimentary normal faults show a NE- to NNE-trending direction of extension similar to that observed on Tinos and Andros (Lecomte et al., 2010). A series of late NNW-SSE trending dykes filled with barite and iron hydroxides cut the mylonites, the cataclases and the two detachments within the same extensional regime (Lecomte et al., 2010; Menant et al., 2013; Tombros et al., 2015). It was shown that these dykes formed during the cooling of the granite once it had entered the brittle field during the latest exhumation steps and that they were fed by fluids convecting between the hot basement and the colder basin brines above (Menant et al., 2013).

The Mykonos laccolith formed through successive magma batches intruding at short intervals and shows different magmatic facies from a pyroxene monzo-granite in the SE to a biotite-monzogranite in the NW, the latter predominating on the island (Lucas, 1999; Lecomte et al., 2010; Denèle et al., 2011). The Delos and Rheneia plutonic facies were studied in detail by Lucas (1999). Mafic enclaves in the core zone testify for a contribution of mantle partial melting during extension and crustal thinning. Most of the intrusion is made of a granodiorite originating from lower crustal partial melting but a component of mantle source is present as well (Pe-Piper et al., 2002). On the Apollonia peninsula, Delos and Rheneia, a planar-linear fabric in the pluton can either result from the orientation of crystals within the flowing magma or by piezocrystallization during cooling. In both cases this planar-linear fabrics was

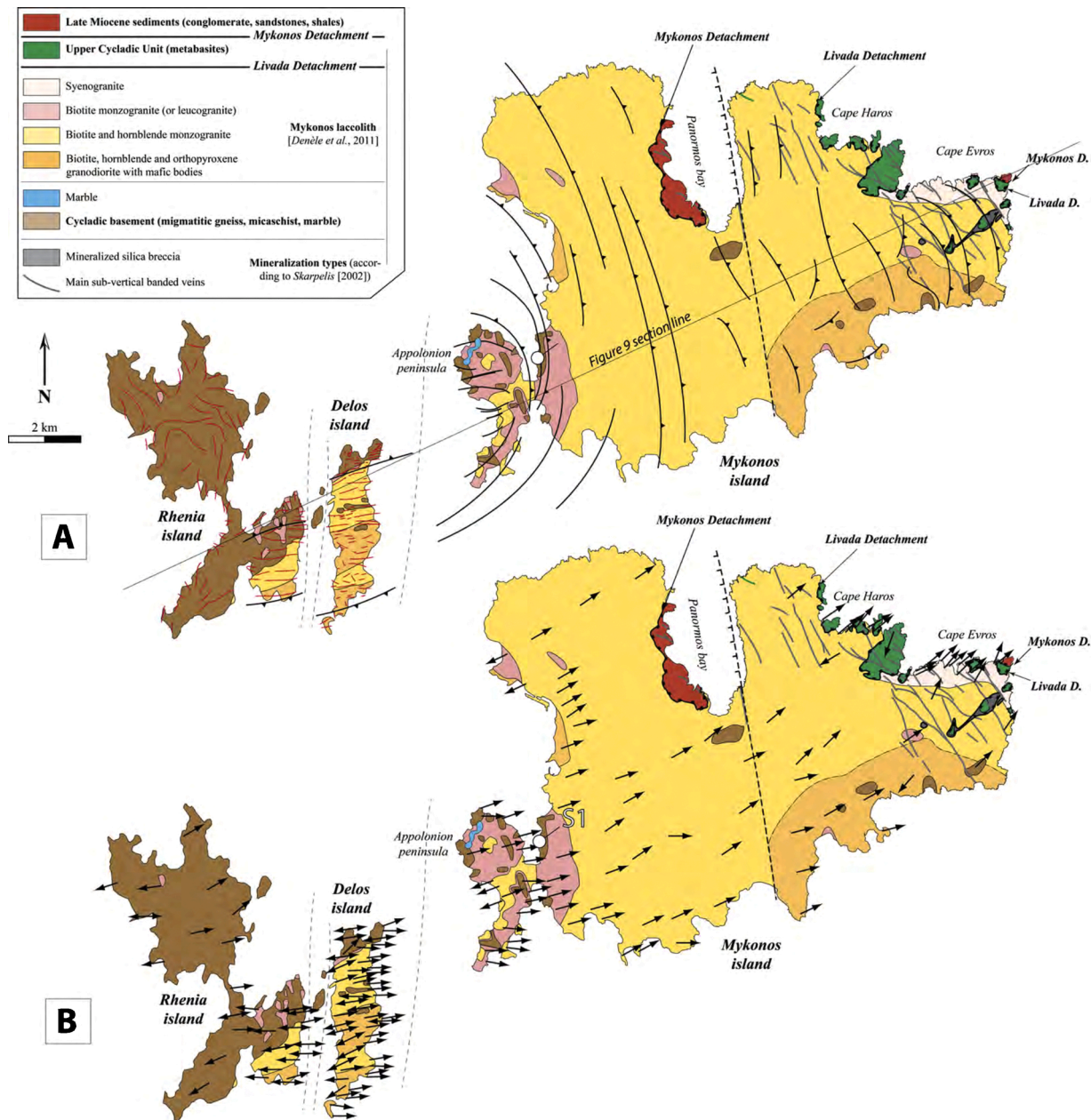


Fig. 3. Tectonic map of the Mykonos-Delos-Rheneia metamorphic core complex. A: foliation trajectories, B: stretching lineations. Compiled after Lucas (1999); Denèle et al. (2011) and Menant et al. (2013).

formed early during the evolution of the pluton (Lucas, 1999). A later study by Denèle et al. (2011) shows that the base of the Mykonos laccolith on the Apollonia peninsula at the contact with the migmatitic dome is diffuse and generally parallel to the ductile fabric and the layering of the migmatites (Fig. 4A). Alternating garnet-sillimanite gneiss, migmatites and granite with large alkali-feldspar phenocrysts mark the contact (Fig. S1), contrasting with the sharp contact associated with contact metamorphism observed in the southern part of the intrusion on Naxos. There, enclaves of paragneiss and marbles of various sizes belonging to the HT dome are included in the granite. Denèle et al. (2011) distinguish four petrographic types within the intrusion: a syenogranite in the northeast near Cape Evros intruding the UCU metabasites and then sheared along the Livada Detachment, a discontinuous biotite monzogranite (or locally a leucogranite) along the basal contact of the laccolith near Apollonia, a biotite hornblende porphyric monzogranite covering most of the island and a pyroxene porphyric granodiorite with mafic enclaves. Lucas (1999) interpret this zonation and the

petrography of the pluton as an inverse zonation, consequence of the drainage of a infra-crustal magma chamber from top to bottom. The intimate link with the migmatite however shows that the plutonic and migmatitic materials were still in the partial-melting field while the granitic magma emplaced. This is in line with the observations of Altherr and Siebel (2002); Altherr et al. (1988) and Stouraiti et al. (2010) that the generation of the Cyclades plutons involves a large component of crustal partial melting. The main source would resemble the biotite paragneiss of Rheneia (Stouraiti et al., 2010).

Few geological maps are so far available for Delos and Rheneia. The first mapping survey was done from 1906 to 1908 and the first map published by Lucien Cayeux (Cayeux, 1911) in the framework of the starting archeological exploration of the Delos sanctuary. It shows mainly granitic rocks with some marble enclaves, amphibolites and gneiss enclaves, covering most of Delos Island and the eastern part of Rheneia, and a large body of "gneiss micacés". A similar map of the two islands was included in the Mykonos Island-Rinia Islands sheet

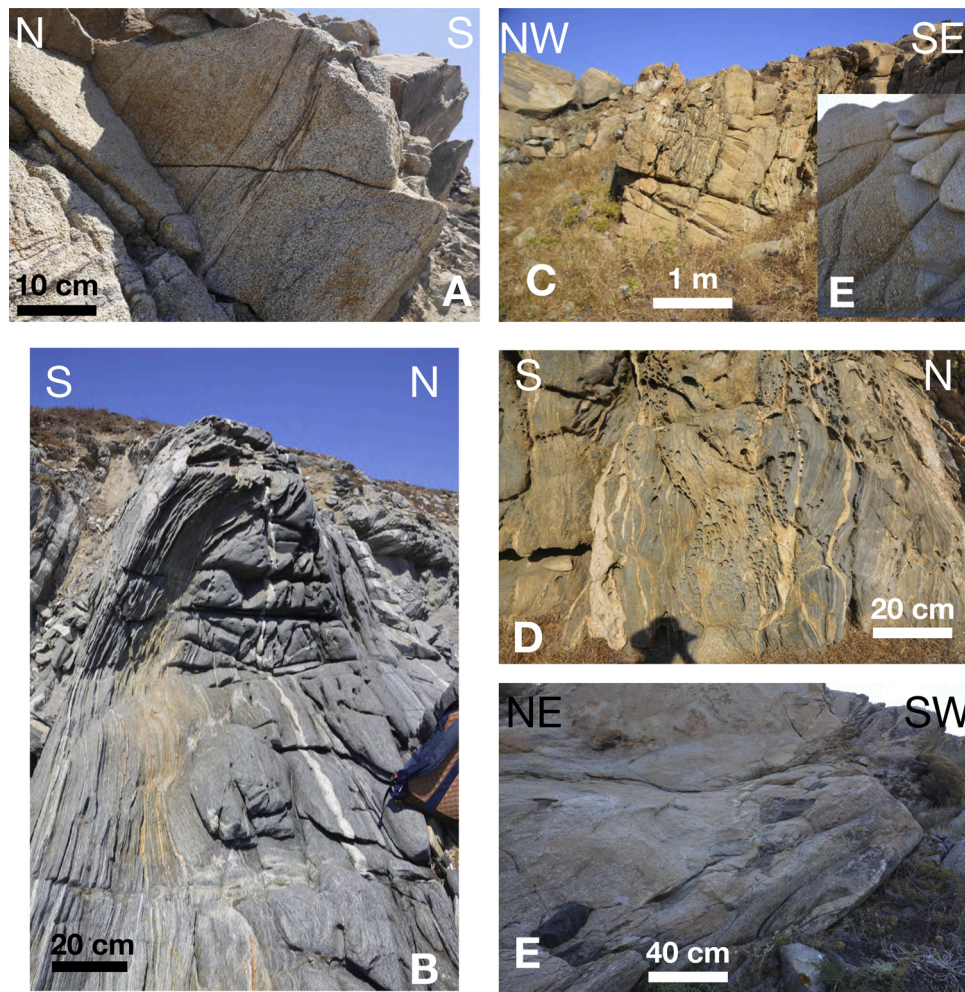


Fig. 4. Photographs of representative outcrops of migmatites and migmatitic gneiss in the core of the Mykonos-Delos-Rheneia metamorphic core complex (see precise location in the supplementary materials). A: diatectic migmatites on Mykonos. B: steep foliation of migmatitic gneiss on Rheneia. C: Steep foliation and alternating migmatites and intrusive granitic dyke on Delos. D: steeply-dipping migmatitic gneiss on Delos. E: gneissic enclaves in the Delos granite. See locations in Fig. S0.

published by IGME (Avdīs, 2004). Pe-Piper et al. (2002) insist on the importance of E–W striking shear zones associated with a steep foliation and horizontal lineation in the center of Delos, which they relate to a component of dextral shear. Denèle et al. (2011) used the map of Delos and eastern Rheneia proposed by Isabelle Lucas in her PhD (Lucas, 1999) showing the distribution of plutonic facies. The only detailed work on the structure and kinematics of deformation is the work of Denèle et al. (2011). These authors show a pervasive E–W trending stretching lineation carried by a low-angle foliation forming open domes in the NW part of Rheneia and a steep E–W-striking foliation in the southeastern part of Rheneia facing Delos where the foliation in the granite is steep and E–W. Denèle et al. (2011) interpret Delos and Rheneia as the root zone of the Mykonos laccolith and put forward three successive episodes of deformation, forceful intrusion in the root zone leading to a prolate fabric, protomylonitization immediately following cooling and finally mylonitization below the detachment.

3. A new geological map of Delos and Rheneia

In this part, we present the results of our field survey on Delos and Rheneia with a new geological map (Figs. 5). Our study is the first one integrating both Rheneia and Delos on single map with a complete survey. Beside a new description of rock facies (Figs. 4 & 6 and supplementary material), our survey leads to the discovery of a new large-

scale shear zone named here the *Rheneia Shear Zone* encompassing a large part of the central island between Ataliothis Bay, the Lazaret and Cape Glaros. The following rock facies are encountered on the map.

3.1. Metamorphic rocks

Migmatitic gneiss, either diatexites or metatexites, and non-migmatitic gneiss (leucocratic or melanocratic) can be described on Delos and Rheneia.

Migmatitic gneiss (Figs. 4, S2–S4) crop out in the northern part of Delos in contact with the granitic rocks and in the eastern part of Rheneia in the core of the dome. Migmatites are also observed as septas of various size inside the main intrusion (Figs. 5, S5, S6). Some of these enclaves are of mappable size reaching up to 200 m in length (Figs. 5, 10). We use here the terminology for migmatites proposed by Maxeiner et al. (2017), modified from Sawyer (2008) and Sawyer and Brown (2008), see also Vanderhaeghe (2001). Both metatexites with a low degree of melting and a preserved cohesion (Fig. S4) and diatexites with a nebulitic texture (Figs. 4, S2) are observed. Diatexites are present both in the core of the dome on Rheneia and within the granite on Delos as large enclaves. *In-situ* concordant (Fig. S3) and foliation-discordant leucosomes are often intensely sheared and transposed in the regional foliation (Fig. 4D). If not associated with an indication of partial melting gneiss are considered non-migmatitic.

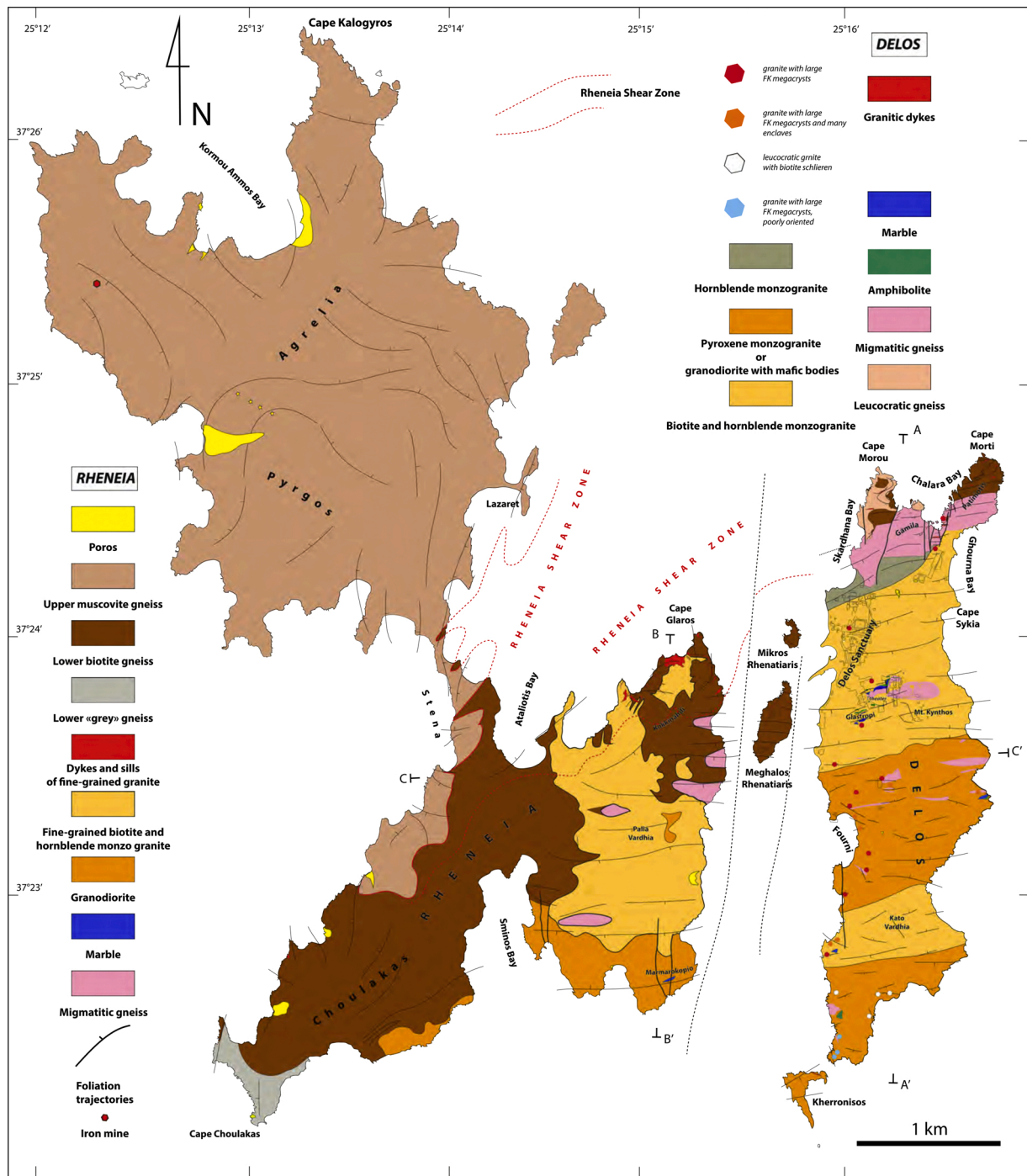


Fig. 5. Geological map of Rheneia and Delos and foliation trajectories. AA' : trace of Fig. 5 cross-section. The map was drawn after our own observations with the addition of the distribution of granitoids on Delos after Lucas (1999).

Biotite melanocratic gneiss with a typical grey patina crop out in the northern part of Delos and in the southern half of Rheneia (Figs. 4B-lower grey gneiss and lower biotite gneiss-, 10, 11, S7), overlying the migmatites. They show a strong layering alternating dark and leucocratic layers. They are often invaded by intrusive aplitic and pegmatitic sills and dykes, more or less transposed by shearing in the Rheneia Shear Zone described below. Variation in biotite modal proportion allows distinguishing grey mica-rich layers from quarto-feldspathic layers giving to the rock a typical banded facies. Quartz and feldspar form compact centimetric layers. Within felsic layers, quartz is abundant and shows undulose extinction and K-feldspars form elongated aggregates. Orthoclase are from place to place infiltrated by worm-like quartz

myrmekite patches. Plagioclase is virtually absent. In more mafic layers biotite forms millimeter unstrained millimetric pristine crystals lying within the foliation without inclusion. Accessory mineral are apatite, titanite, zircon and tourmaline.

Gneiss is also observed as enclaves within the massive granite (Figs. 4E, 6 E, S3C, S5, S6, S15). Those brownish gneiss form either the bulk of small metric lenses or are associated with interbedded marble and amphibolite/pyroxenite layers within larger few hundred meters long enclaves. These gneisses have a characteristic brown patina due to a higher proportion of biotite compared to banded migmatitic gneiss. Micaceous layers are thicker compared to felsic material forming lenticular sheet giving the appearance of an augen-gneiss defined by

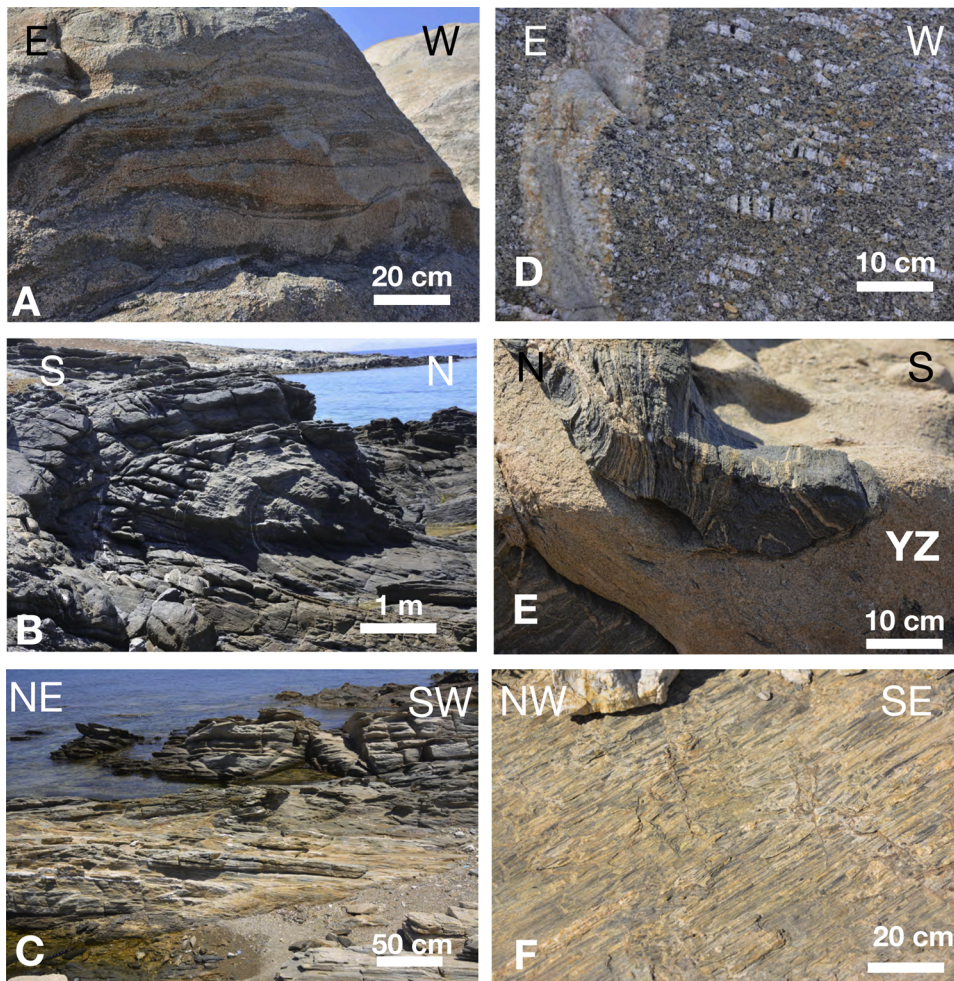


Fig. 6. Photographs of representative outcrops in the Mykonos-Delos-Rheneia metamorphic core complex (see supplementary materials for precise location). A: alternating facies with low-angle foliation in the Delos granite. B: example of a large synfolial fold with its axis parallel to the regional stretching lineation. C: Muscovite-bearing leucocratic gneiss and similar folds with shallow-dipping axial planes and NW–SE trending axes. D: Later dyke cutting the foliation marked by the orientation of feldspar megacrysts in the Delos granite. Extension responsible for the dyke opening is parallel to the stretching in the granitic magma. Note the cracks in feldspar megacrysts filled with late magmatic fluids, here tourmaline. E: folded gneiss enclaved in the Delos granite. F: Stretching lineation in the Rheneia biotite melanocratic gneiss. See locations in Fig. S0.

almond-shaped quartzo-feldspathic nodules. These rocks with more than 50% biotite with a compositional layering are interpreted as aluminous paragneisses.

Muscovite leucocratic gneiss covering most of the northern half of Rheneia (Figs. 5 -upper muscovite gneiss-, S9). These gneiss are described as migmatitic in Denèle et al. (2011). They are made of an alternation of beige fine-grained gneiss with white micas and whitish layers with a more feldspar-rich composition. Our new observations suggest instead that these white layers are not leucosomes but correspond to the complete transposition of acidic dykes rich in quartz and feldspar intruded within pelitic micaschists during the formation of the Rheneia Shear Zone (Fig. S9). The interface of the two gneiss types is observed on Rheneia along the narrow isthmus separating the northern and southern halves of the island (Figs. 6C, S8). Within the contact zone an intense layering results from shearing in the core of the Rheneia Shear Zone.

Amphibolites are observed in enclaves highly variable in size, from a few centimeters to several tens of meters, within the granitic rocks. The largest one are found on Delos on Ghlastropi hill (Fig. 5) overlooking the antique theater and in the southern part of the Delos pluton. At Ghlastropi and on a cape southeast of Mount Kynthos, they are associated with coarse-grained marbles (Fig. S10). Marbles crop out as large enclaves within the pluton, either with amphibolites or alone. Their grain-size is variable but usually coarse, reaching several cm southeast of Mount Kynthos. The latter outcrop shows a close association of the coarsest-grained marble with a large chunk of amphibolite. The contact of the marble with the amphibolite is marked with skarn layers, a few tens of cm thick, with garnets and pyroxene. The skarn garnet is made of

xenomorphous andradite (Adr90-80Gr10-20) and the pyroxene layer of hedenbergite (Hd20-40Dio80-60), with scattered massive crystals of vesuvianite (Cayeux, 1911). Amphibolite and marbles show a common strong foliation and a stretching lineation, and late veins formed in the conditions of the greenschist-facies cut the amphibolite, indicating the same direction of stretching, parallel to the regional extension. The long axis of the lenses is generally NE–SW, which is the main stretching direction in the island and the dip of bedding is variable.

Field relations show that the non-migmatitic gneiss are not the deformed equivalent of the migmatites and that, instead, they correspond to the partially molten core of a dome otherwise not molten. The migmatite, either metatexites or diatexites show the classical duality between leucosomes and restites, and the cohesion of the foliation is lost in the diatexites. Surrounding gneiss, instead, do not show any trace of partial melting and they are intruded by granitic dykes and sills not produced locally. High shearing strain of these gneiss and intrusive dykes leads to banded gneiss with acidic lithologies that do not correspond to former leucosomes.

3.2. Plutonic rocks

The categories of granitoids identified on the map are based on the detail study of Lucas (1999). Two predominant facies are observed (Figs. 6, S11). A first facies is composed of a monzogranite containing biotite, hornblende and pyroxene, it often includes mafic enclaves. They outcrop in the central part of the pluton in Delos and Rheneia and marginally in Mykonos and form as a whole around 15% of the granitoid outcrops. Pe-Piper et al. (2002) describe the same rock as granodiorite.

The second facies is also a monzogranite with biotite and hornblende but without pyroxene. It constitutes the main body (80%) of Mykonos-Delos Rheneia pluton. Numerous aplitic and subsidiary pegmatitic dykes intrude the biotite gneiss in the vicinity of the contact with the granite (Figs. 7, 8, S13). Several generations are observed, more or less affected by the deformation showing their syn-kinematic character. The earlier dykes are folded and transposed parallel to the regional foliation while others with similar composition intrude these folded ones and are less deformed. Fig. 7D shows an acidic dyke cutting the foliation of the host gneiss and itself stretched along the same direction. Figs. 8A shows highly sheared dyke totally transposed parallel to the regional foliation and then folded. Fig. 8B shows three generations of acidic dykes. The oldest are strongly sheared and transposed. The resulting gneiss is then cut by a new dyke, which is itself stretched (here the YZ plane is shown so that the stretching is not visible). A third pegmatitic dyke, less deformed cut through the two earlier generations. These observations show that the various generations of dykes are emplaced during the deformation process. Dykes are also observed within the intrusion. Fig. S13B shows a dyke oriented E–W with fuzzy boundaries and evidence for fluidality of the granitic magma in the southern part of the intrusion on Delos where mafic enclaves are observed in large numbers and the granite poorly oriented. It shows that deformation was active while the pluton was partly consolidated and injections continued.

The massive I-type granitic pluton that crops out over a large part of Delos, from the center to the south has a phaneritic texture. The density of mafic enclaves increases southward. The main body of the pluton consists essentially of amphibole-biotite-bearing granite with large K-feldspar megacrysts. It is the dominant facies in Mykonos (Fig. 6). The tabular K-feldspar crystals vary in size (from few millimeters up to few centimeter) and modal proportion within a coarse to medium grained groundmass of plagioclase, quartz and mafic mineral such as amphibole coexisting with variable amount of biotite. In Delos, amphibole granite without biotite is observed south of Ghourna bay and Kato-Skardania towards the northern contact with migmatitic gneiss. They are leucocratic with a pink patina and are titanite-rich. Such a facies is also found in Mykonos to the west of Appolonia peninsula and sporadically in Rheneia in the eastern peninsula at the contact with the gneiss. Finally

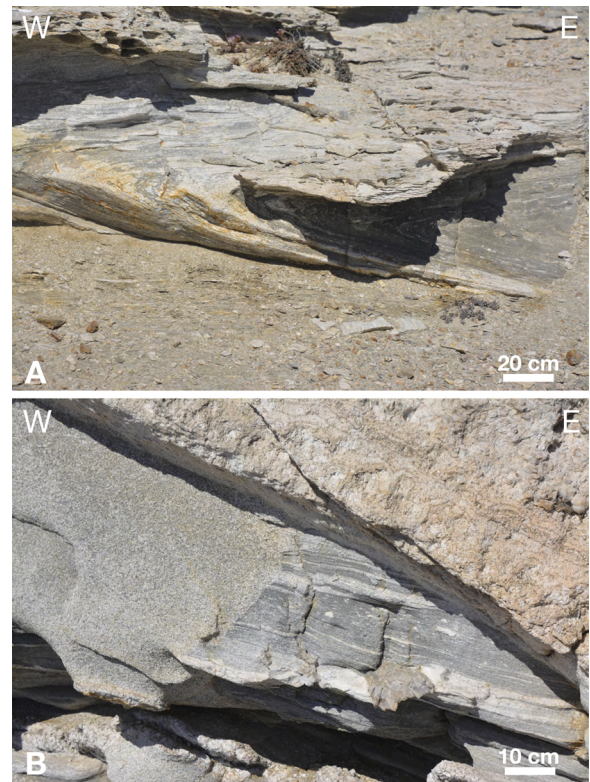


Fig. 8. Progressive deformation of dykes within the Rheneia Shear Zone on Rheneia. A: Syn-folial folds affecting already transposed dykes. B: three generations of dykes with different grain size in the YZ plane. All three generations show stretching in the perpendicular direction. Location on Fig. S0.

biotite granite without amphibole in Delos is observed as a discontinuous layer, tens meter thick, at the contact with the northern migmatitic gneiss conformable with gneissic structure. Note that this ordinary granite without amphibole forms also late intrusion found essentially within the dyke complex intruding migmatitic gneiss in the northern

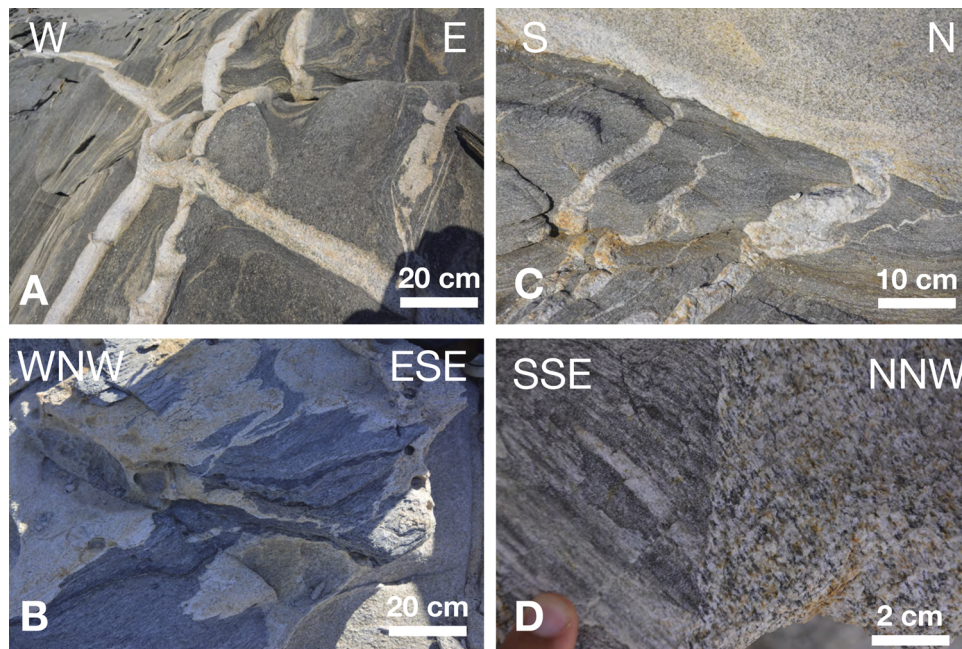


Fig. 7. Several generations of dykes intruding the biotite gneiss on Rheneia, within Rheneia Shear Zone. The older the dyke, the more deformed it is but the stretching direction is constant. Location on Fig. S0. See locations in Fig. S0.

part of the island. It is found as well as a particular facies within the amphibole porphyry granitic pluton such as in the southeast contact of the marble-amphibolite enclave southeast of Mont Kynthos. Orthoclase varies between 25 and 30%, plagioclase 18–26% and biotite 20–22%. Accessory phases are magnetite, ilmenite and titanite. Whatever the respective abundance of amphibole and biotite, quartz never exceeds 30% and K-feldspar (orthoclase) dominates over or equals plagioclase modal proportion. According to the IUGS nomenclature (Streckeisen, 1975) the rocks can be classified as low-silica high-K granite with some variations close to the field of granodiorites. Accessory minerals are zircon, titanite, apatite, red-brown pleochroic allanite, magnetite, and ilmenite. Titanite with its typical high relief diamond-shaped cross-sections may be abundant especially in amphibole granite without biotite. Zircon is widespread and included both in felsic and mafic minerals. K-feldspar (Or81-93Ab17-06An02-01) may include euhedral plagioclase (An43-19Ab55-79Or2-1) and mafic minerals. Amphibole is a green/brown hornblende scattered throughout the section or forming aggregates. Biotite is an Al-poor biotite (X_{Mg} 46–39, 3.2–4.3% TiO₂).

In more detail, close to the contact with the northern migmatitic gneiss to the east, the granite shows locally abrupt textural variation from isotropic texture to foliated gneissic texture. Such a gradual contact is particularly striking along a fault located between Gamilla Hill in the west and Patiniotis peninsula in the east (Fig. 5). From south to north, the porphyritic amphibole-biotite granite passes to migmatitic gneiss over approximately 20 m. First, the proportion of orthoclase megacrysts increases drastically, forming more than 50% of the rocks volume with alignment of elongated crystal along their c-axis in a plane parallel to the gneiss foliation. Then, the granite forms residual lenses and disrupted sills within massive feldspar-rich or micaceous gneiss. White aplite veins within the northern gneiss show a saccharoid texture dominated by deformed K-feldspar and quartz. Pegmatitic veins are dominated by quartz. These veins, less than 1 m wide, are observed in the extreme north of the northern gneiss. They contain centimeter-size crystals including either muscovite or tourmaline.

Pyroxene monzogranite or granodiorite outcrop in the central part of Delos pluton. They have a porphyritic texture but are distinguished from the monzogranite described above by significantly lower proportion in K-feldspar megacrysts. They also stand out for their mafic magmatic enclaves showing variable size (metric to decametric), shape and composition (gabbro, diorite, monzodiorite). Note that those mafic enclaves, witnessing the presence at depth of a mafic magma, are largely present almost everywhere but are more numerous in the southern part of the Delos granite, in a region where the pluton is less oriented. These pyroxene-bearing granitoides are leucocratic (with up to 70% quartz-plagioclase-K-feldspar where plagioclase + feldspar dominates over quartz) and contain biotite, amphibole and pyroxene. Accessory minerals are allanite, apatite and titanite. Quartz proportion varies between 16 and 27%. Feldspars with orthose composition range from 6.4–18% while plagioclases (labrador to oligoclase) vary between 28–45.6%. Biotites, up to 16% in modal proportion, dominate over amphibole and shows variable Al/Mg contents especially in granodioritic facies while in monzonitic one it has lower and rather constant alumina content. Amphiboles vary between 1.7 and 8% in modal proportion. They are ferro-pargasite in the monzonitic facies and ferro-edenite in the granodioritic one. Pyroxene shows variable proportions (from 0.5 à 12.5%) somewhat complementary with amphibole one and has a ferro-diopside composition whatever the facies.

Leucogranite is observed exclusively in the south of the island southwest from Kato-Vardia and are associated with pyroxene monzogranite/granodiorite described above. The medium to fine-grained rock contains up to 45% quartz, up to 35% K-feldspar and less than 10% plagioclase and biotite. Pegmatitic layers are exclusively formed by coarse quartz and K-feldspar and include tourmaline in spherical aggregates.

Ordinary granite (feldspar, quartz and biotite) without amphibole is fine to coarse-grained and show an aphaneritic texture. It may be

sometime porphyritic when orthoclase crystals are more than 1 cm long. These are late granites found essentially within the dyke complex intruding migmatitic gneiss in the northern part of the island. It is also found as a particular facies within the amphibole porphyry granitic pluton such as in the southeast contact of the marble-amphibolite enclave southeast of Mont Kynthos. Orthoclase varies between 25 and 30%, plagioclase 18–26% and biotite 20–22%. Accessory phases are magnetite, ilmenite and titanite.

The distribution of metamorphic enclaves within the pluton is irregular. The largest enclaves (several hundred of meters long) made of gneiss, migmatites, amphibolites or marbles are found in the center of Delos and around the sanctuary (Fig. 5). It is not clear whether these large enclaves in fact correspond to screens and shear zones between different intrusions as proposed by Pe-Piper et al. (2002) because the transitions between the different facies of the granite are often gradual. We rather interpret them as septas of the surrounding gneiss and of the CBU enclosed in the magma as it rose toward the surface and was deformed (Fig. S14) but more detailed studies would help answering this question. They show the same stretching direction as the granite and the gneiss around it. Their deformation was likely acquired before they were enclaved in the granite and continued afterward with the same general E–W stretching as shown by the example of the metabasites associated with the marble SE of Mount Kynthos. Mafic enclaves witnessing the presence at depth of a mafic magma are largely present almost everywhere but more numerous in the southern part of the Delos granite, in a region where the pluton is less oriented.

3.3. Sedimentary rocks

Outcrops of sedimentary rocks are very limited on Delos, Rheneia and Mykonos and primarily correspond to recent deposits. Beach rocks have been recognized along the western coast of Delos (Desruelles and Fouache, 2007) and correlated with the ones of Rheneia and Mykonos (Desruelles et al., 2009), they correspond to different level stands of the middle Holocene and show a relative subsidence of 4 m of the western central coast of Delos during the last 5000 years. Onshore, the deposits of the three islands are more variable.

In Delos, only two clear outcrops exist, one (P1) between the sanctuary and the gymnasium (Fig. S15 A) and one eastward of Fourni bay. The initial extension of P1 may have been larger before exploitation and extended to the western coast, alluvial deposits seems to extend south-westward toward the Archégèsion zone which is covered by about 1 m of thick calcareous sandstone. The earthwork done while building the temples caused the outcrops to disappear however remnants of these deposits are visible on the underlying granite in some buildings. The island morphology is compatible with a depot center in the valley that flows westward but, today, the continuity cannot be established between P1 outcrops and the coast. The matrix is calcareous and detrital clasts consist mainly in quartz and granite pebbles, poorly sorted and angular.

In Rheneia, in addition to the beachrocks, larger outcrops of recent sediments can be observed within the bed and mouths of small creeks. They can extend up to a few hundred meters from the coast but are restricted to the creek valleys. Facies are highly variable, from slope breccia and coarse calcareous conglomeratic sandstones to fine grained levels with cross-bedding (Fig. S15 B, S15 C) suggesting an alternation of fluvial and nearshore influences. Thin-section observations confirm the marine setting of the fine grain levels where algae and foraminifera are numerous, detrital clasts have very local origin (granite, quartz, plagioclases). The presence of this kind of facies is rather common in the Mediterranean since the drastic sea level drop during the Messinian resulted in deep fluvial valleys later filled by fluvial and/or marine sediments during the Quaternary. It is worth keeping in mind that the three islands, Mykonos, Delos and Rheneia were connected and parts of a much larger island including Andros and Tinos during the last glacial maximum 21 ka ago (Simaiki et al., 2017). The rather fast sea level

changes during the Quaternary glaciations favored such intercalations fluvatile/paleosol and shallow marine.

4. A cross-section through Rheneia and Delos

Fig. 9 shows an E–W cross-section through the southern part of Rheneia and the central part of Delos and two N–S cross-sections through Delos and Rheneia (see location of Fig. 5). It highlights the geometrical relations between the different lithologies described above. The core of the gneissic structure is occupied by the migmatites as illustrated on cross-sections BB' and CC'. However, because of the folds with E–W axial planes, the contact between the migmatites and the granites can locally be vertical or even overturned, with the migmatites on top of the gneiss, as shown in the northern part of Delos (section AA').

The migmatites crop out on Rheneia thanks to antiforms with E–W axes and steep axial planes (Figs. 5,9, S2). These migmatites also flank the Delos monzogranite along its northern boundary between Skardhana and Ghourna Bays (Figs. 5,9A, 13, S4) and they appear as large enclaves within Delos granite (Figs. 5,9A, S5). The migmatites are overlain in the core of the dome by the biotite-rich gneiss that crop out in the southern part of Rheneia and the northernmost part of Delos. The contact between these two lithologies is often fuzzy with a progressive transition and some recurrences of one facies within the other (Fig. S8). On top of the biotite-rich gneiss, the muscovite gneiss makes most of the northern half of Rheneia and part of Cape Morou peninsula on Delos. The contact between the two gneissic lithologies is made of regularly alternating dark and leucocratic gneiss in a zone where all early contacts, including dykes and sills are totally transposed in the regional foliation by the

activity of the Rheneia Shear Zone (see description below) (Fig. S8).

The granites intrude the gneissic dome as sills, in the migmatitic gneiss and the biotite-rich gneiss, which are also observed as large enclaves and the intrusive contact is folded by the folds with E–W axial planes. The northern parts of Delos and of the southeastern peninsula of Rheneia are invaded by acidic dykes around the limits of the pluton. These aplitic and pegmatitic dykes are intensely deformed within the Rheneia Shear Zone (Figs. 12,13) that was active during their emplacement. The foliation within the granitic intrusion is parallel to the foliation in the gneiss and the migmatites.

The overall geometry shows a series of antiforms and synforms with E–W striking axes, almost horizontal on Delos and eastern Rheneia and slightly west-dipping in the central and western part of Rheneia, topped with the shallower-dipping gneiss of west Rheneia and northern Delos forming a gentle dome. Folds are open in the upper part of the dome and tighter in the deeper migmatitic gneiss. The axes of these tight folds seen in the migmatites plunge westward underneath the gneiss with a shallower west-dipping foliation of western Rheneia. The main foliation on the map thus appears with an E–W strike in the core of the dome and with a N–S strike in the western part.

5. Progressive deformation and syn-kinematic intrusions within the Rheneia Shear Zone

The entire region of Rheneia and Delos Islands is affected by intense deformation with evidences of strain gradient across major shear zones. Both the gneiss and the intrusions show a progressive deformation characterized by a single consistent E–W stretching direction (Fig. 6F) as

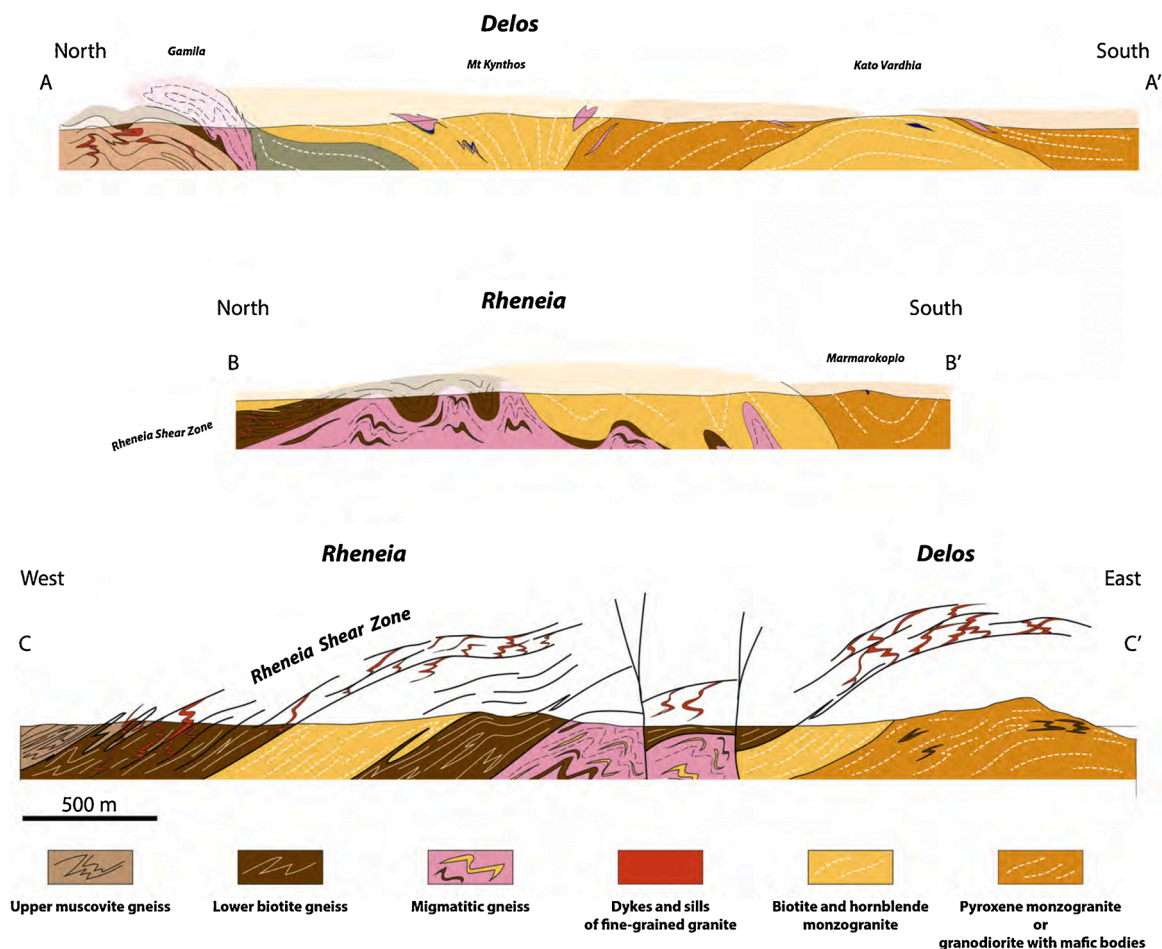


Fig. 9. North-South cross-sections AA' and BB' through Delos and Rheneia, respectively, and E–W cross-section through Rheneia and Delos (location on Fig. 5). No vertical exaggeration. Foliation and sheared dykes are represented above the section to show the extent of the shear zone and its larger-scale geometry.

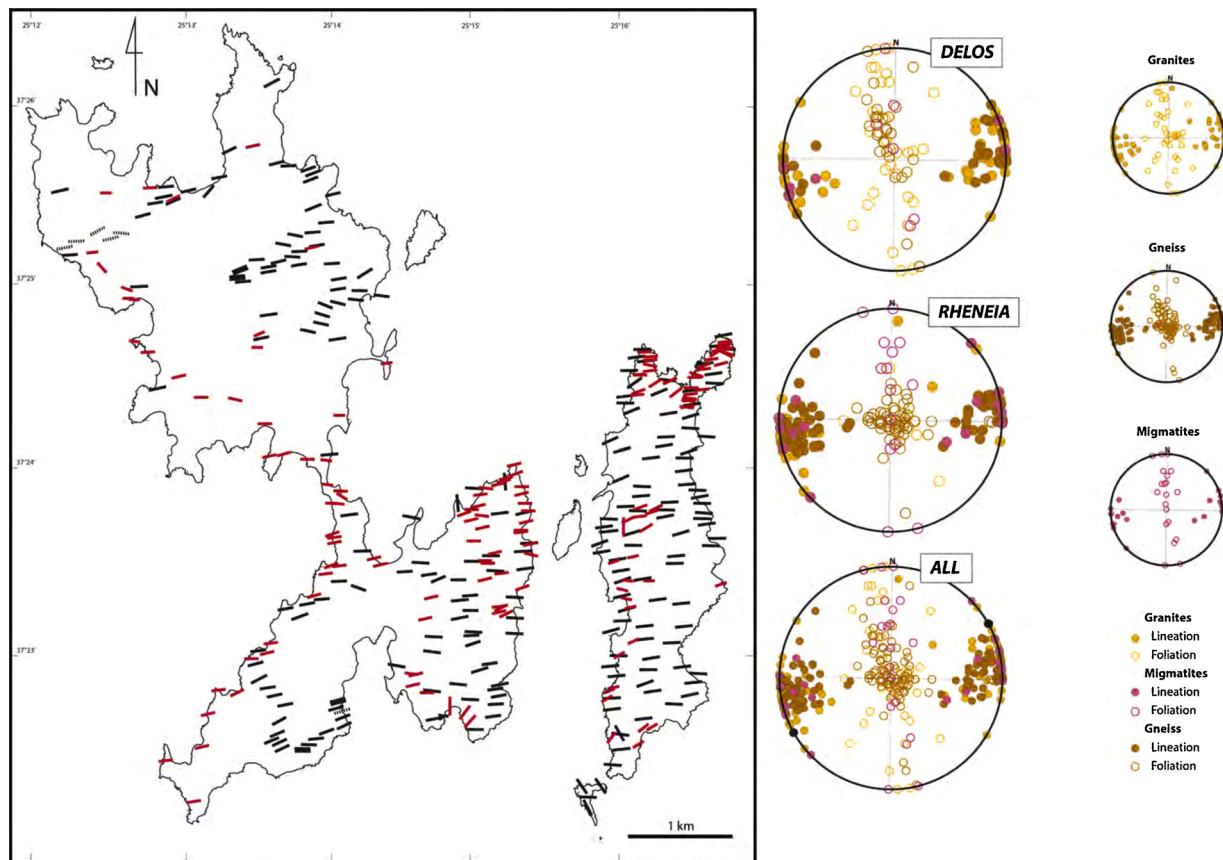


Fig. 10. Map of stretching lineations on Rheneia and Delos and stereograms of foliation poles and lineations. Black lines: stretching lineations after Lucas (1999) and Denèle et al. (2011). Red lines: stretching lineations after our own observations.

shown by the lineation map and stereograms of Fig. 10. This stretching lineation is carried by a foliation organized around folds with axes that trend parallel to the direction of the stretching lineation (Figs. 6B, S7). Poles of foliation are organized within a vertical plane striking $\sim 160^\circ$ E perpendicular to the average trend of the lineation, in all three main facies, granitic rocks, gneiss and migmatites and with the same geometry on Delos and Rheneia (Fig. 10). This geometry is due to folding with axes parallel to the stretching direction. The foliation shows low dip in most of the northern half of Rheneia and it becomes steeper in the south-eastern part of the island facing Delos (Fig. S2). On Delos the foliation is steep in the center of the island in the vicinity of the sanctuary (Fig. S4) and further south and it becomes shallower toward the north and the south. The steep foliation observed in the migmatites is due to folds with steep E–W-striking axial planes observed along the eastern coast of Rheneia and in the southeastern peninsula (Fig. S2). The homogeneity of the granitic lithologies on Delos makes the observation of such folds difficult because of the absence of alternating compositions and because there is no original strong planar anisotropy in the non-deformed granites, but, when present, the foliation and the lineation have a similar attitude as in the gneiss. Smaller-scale folds are observed in the gneissic basement and in the marble lenses, in the migmatites as well as in the enclaves within the granite (Fig. S16). Most of these ductile synfolial folds show axes parallel to the stretching lineation but locally they display more N–S axes (Fig. 6C).

One thus observes three types of folds: the first folds to form are synfolial folds seen at small scale in all lithologies with axial plane parallel to the main foliation. The orientation of their axes is not easy to measure but some of them are E–W and other, less frequent are oblique, closer to N–S. The regional foliation is then folded by open folds with E–W axial planes in the upper part of the edifice. These folds are visible at map scale on Rheneia and Delos. They affect the gneiss, the

migmatites and the foliated granites. In the core of the structure the foliation is folded by folds with steep limbs and E–W-striking vertical axial planes. These folds are most of the time not recumbent but in the northern part of Delos, the migmatites of the core of the dome are seen above the biotite melanocratic gneiss. All these folds have their axes parallel to the stretching lineation and thus result from a high component of shearing that has transposed all structure parallel to the main shearing direction. All these folds, including the early synfolial ones, could have formed in a single continuum of shearing, but accurate dating would be necessary to be more conclusive on this matter. If we assume that, indeed, the folds belong to a single continuum of deformation, then the early synfolial folds should be seen on an E–W cross-section at large scale, as represented on Figs. 9C and 11. The configuration of the coastline is however not favorable for continuous observations along an E–W section.

The stretching lineation is pervasive and its direction consistent over the whole studied region (Fig. 10). It is marked by the elongation of enclaves in the granite and the alignment of K-feldspar phenocrysts in the foliation (Figs. S3, S11, S12, S13, S14, S17). In the gneiss it is marked by the alignment of micas aggregates and the stretching of feldspar grains, the boudinage of aplitic dykes. A prolate fabric in the aplitic dykes also marks this well-organized stretching with a strong lineation visible in the XY foliation plane and the XZ plane, but no visible fabric in the YZ plane (Fig. S18).

Clear kinematic indicators in the XZ plane are not frequent. Those we could observe indicate a top-to-the east sense of shear shown by sigmoidal foliation and asymmetrically boudinaged dykes in the muscovite-gneiss of Rheneia (Fig. S17) or sheared dykes on Delos (Fig. S12D & S12E), but at least one local observation shows the opposite sense on Delos (Fig. S12 C).

The progressive deformation of the aplitic dykes shows intense

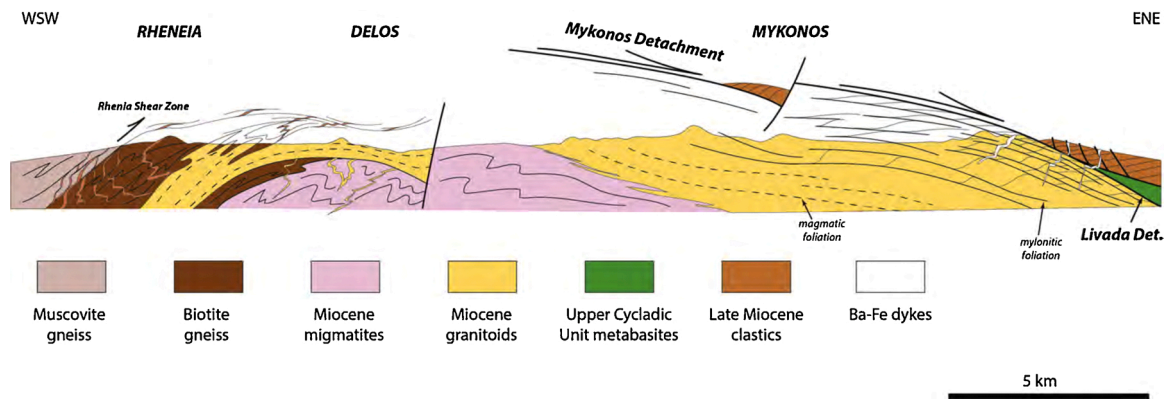


Fig. 11. Synthetic cross-section through Rheneia, Delos and Mykonos, from the migmatitic core to the supra-detachment basin. No vertical exaggeration.

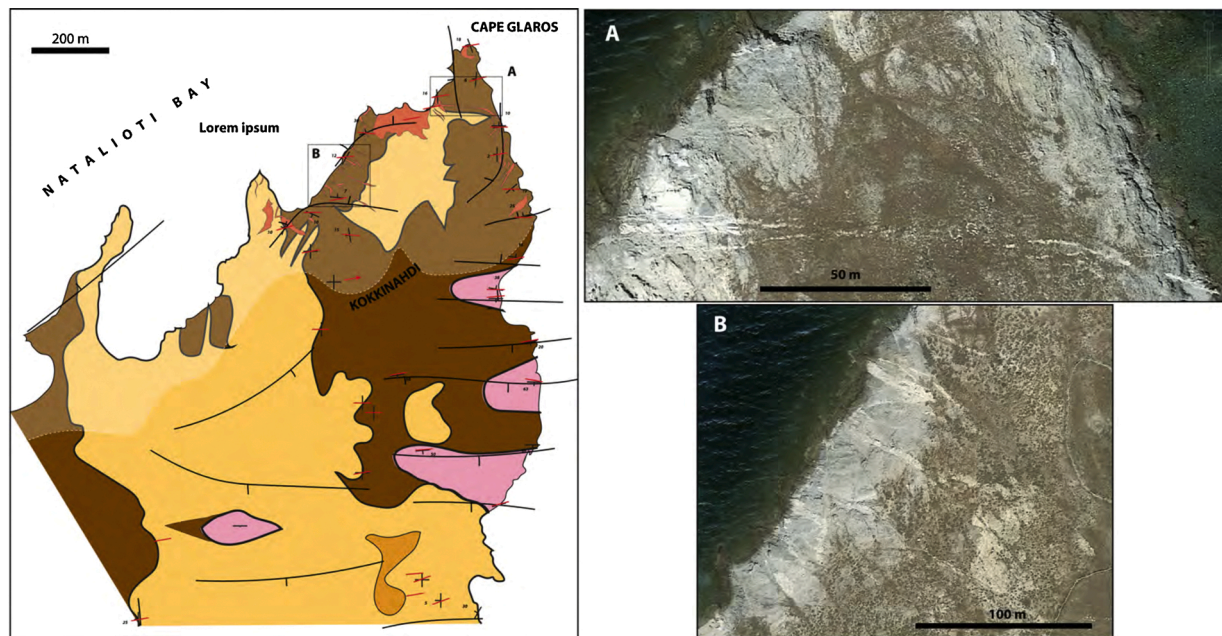


Fig. 12. Detail of the geological map of Fig. 4 showing the extent of the Rheneia Shear Zone and the largest mappable acidic dykes. A and B: satellite images of the largest dykes (Google Earth).

folding and shearing in the gneiss above the granite and the migmatites as well as along the contact between the biotite-gneiss and the muscovite gneiss (Figs. 8,10,12,13). This thick shear zone is hereafter named the *Rheneia Shear Zone*. Figs. 7 and S12 shows several generations of dykes with variable grain-size progressively deformed within the shear zone in the course of their intruding the gneissic basement. The direction of stretching is the same in the host rock and in the dykes and the older dykes are progressively transposed by shearing and folding within the regional foliation. This suggests that the alternation of acidic and gneiss layers in the muscovite gneiss and in the contact zone is a consequence of the activity of the Rheneia Shear Zone. The shear zone can be followed all along the northern coast of the southeastern peninsula of Rheneia, from the isthmus, to Natalioti Bay and then to Cape Glaros (Figs. 5,12). It can be followed also northward along the east coast of Rheneia, at least to the latitude of the Lazaret (Fig. 5, Fig. 10) where the small peninsula attached to main island with a tombolo displays intensely deformed gneiss with spectacular synfolial folds. The Rheneia Shear Zone can then be observed on Delos in the gneiss injected by dykes from the coast of Skardhana Bay to Cape Morou and Patiniotis Peninsula (Fig. 13). The continuity of the shear zone across the narrow strait between Rheneia and Delos is not ascertained, but the position of the shear

zones with respect to the granite observed on either side is similar and the distance is short compared to the magnitude of the shear zone. We thus consider that we have the same shear zone on the two islands. The intensity of folding and dyke transposition indicate a strong flattening associated with the evolution of the Rheneia Shear Zone. Whether or not this flattening was achieved within a regional non-coaxial flow is not known with precision but kinematic indicators we observed suggest a top-to-the east sense of shear (Fig. S17). The presence of synfolial folds with axes parallel to the stretching lineation would however suggest a strong component of simple shear within the shear zone (Fig. S7).

Most of the basement enclaves show a foliation and stretching lineation parallel to the regional ones and to those observed within the intrusion suggesting a common weak rheology in both materials. Locally however some more abrupt contacts are however observed. Figs. 6E and S14B show a typical case where folded gneiss enclaves with sharp limits are included in a fine-grained granite, itself intensely stretched. It shows that this part of the intrusion was injected after an intense deformation of the host gneiss that had already cooled to behave more rigidly. This observation reinforces the notion of a continuum of deformation and intrusion during a protracted period and not as a single intrusion.

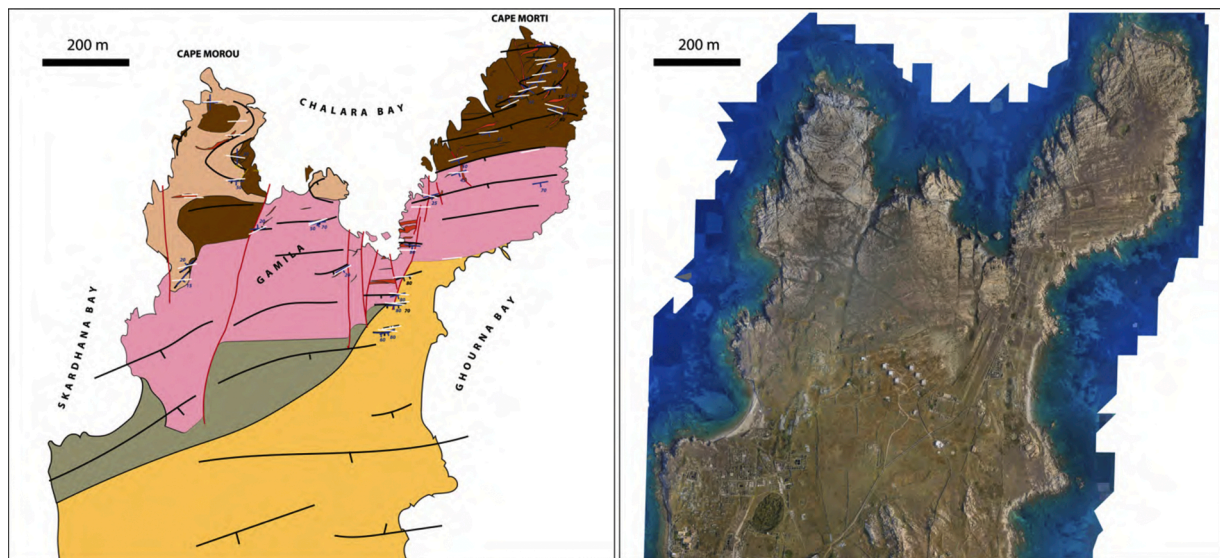


Fig. 13. Detail of the geological map of Fig. 4 on Delos showing the contact of the granite and the gneiss, with the intervening migmatites and the largest acidic dykes. Right: Drone image of the same region (image Iconem-EFA).

6. The Mykonos-Delos-Rheneia MCC and the NCDS

The geometry and kinematic data presented above complete our knowledge on the Mykonos-Delos-Rheneia MCC so far mostly limited to the large intrusion that roofs the topmost parts of the migmatite dome on Mykonos, except for the works of Lucas (1999) and Denèle et al. (2011). Fig. 11 shows a schematic cross-section through the whole MCC, from the muscovite gneiss along the western coast of Rheneia to the Mykonos Detachment and the Late Miocene supra-detachment basin cropping out in the northeast of Mykonos. The migmatite dome crops out from the east of Rheneia to the Apollonia peninsula in western Mykonos. As discussed in Denèle et al. (2011), the composite Mykonos laccolith roots within the dome in Delos and Rheneia. On the cross-section, the strike-slip faults inferred on the geological map along the Delos Strait have been simplified for the sake of clarity but they indeed offset laterally and vertically the gneiss-granite contact. Only one late fault is shown between Mykonos and Delos. The core of the dome is not affected by the brittle deformation associated with the detachment, but it has recorded the ductile E–W stretching and folding before and during the emplacement of the pluton. The N–S evolution of the attitude of foliation on Delos shows large-scale undulations with axes parallel to the regional stretching as well. These fold with their axes parallel to the stretching direction relate to a component of N–S shortening (constriction).

The fabric associated with the E–W stretching is thus observed in all lithologies, from the migmatites to the gneiss and the intrusive granites. It is active at high temperature in the migmatites and in the intrusions at the magmatic stage and continues in lower-temperature conditions in the amphibolitic enclaves showing greenschist-facies stretching. It was thus active during the exhumation of the core of the dome. As proposed earlier by Faure et al. (1991), the direction of stretching is parallel to the long axis of the dome, like on Naxos, thus making the MDR a a-type MCC (Jolivet et al., 2004a, 2004b).

The enrichment of the intrusion in mafic enclaves toward the south, and the loss of a strong fabric may suggest that the roots of the pluton are in the southern part of Delos and Rheneia, a situation that can be compared to the Serifos pluton (Rabillard et al., 2015). Previous studies concluded after Lucas (1999) that the root zone was in the center of Delos because the foliation is steeper there (Denèle et al., 2011) but the attitude of the foliation is for a great part due to late folding during exhumation and the root zone is wide. The deformation recorded in the migmatites continued during the emplacement of the pluton with the

same direction of stretching and the same general geometry of folding. Folds with E–W axes and steep axial planes are observed both in the migmatites and in the granite itself where the foliation attitude varies from vertical to horizontal with a very consistent E–W trending lineation as shown on the map of Figs. 3 and 9. The geometry of folds however evolves from deep to more superficial levels. The detachment itself and the silicified breccia underneath are folded with axes parallel to the stretching direction and the folds are broadly open, while the migmatites and the granite display tighter folds and steep foliations in the core of the dome. This same observation can be made in the larger dome of Naxos (Kruckenberg et al., 2011).

The Rheneia Shear Zone extends from Rheneia to Delos but is not observed on Mykonos that is structurally higher. Its general dip is toward the west. The sense of shear has been drawn top-to-the east on the cross-section based on the kinematic indicators we could observe but this remains to be ascertained. It has certainly accommodated an intense flattening and an intense non-coaxial shearing as illustrated by the presence of folds with axes parallel to stretching, but a component of shear with the opposite sense would not be illogical given the general attitude of the shear zone with its westward dip. The Rheneia Shear Zone can thus be either a tilted top-to-the east shear zone accommodating a part of the general shearing deformation associated with the detachment, or a conjugate shear zone accommodating the rising of the dome in the footwall of the detachment.

7. Discussion, evolution of the MCC

The complete cross-section from Rheneia to Mykonos thus shows the progressive stretching of the crust from the formation of a lower crustal migmatitic dome and its exhumation, to the syn-tectonic intrusion of a granitic laccolith in ductile conditions in the core of the dome and the progressive shearing of the upper part of the system, including the laccolith by the NCDS, first in ductile conditions (Livada Detachment) and then in brittle conditions (Mykonos Detachment), until the deposition of a supra-detachment basin in the Late Miocene and emplacement of a system of baryte and iron hydroxide dykes during cooling and late brittle deformation (Fig. 14). This continuum preserves the same stretching direction all along the exhumation process (e.g. Lecomte et al., 2010; Menant et al., 2013).

Fig. 15 shows a kinematic evolution in four stages along this cross-section. The general situation is similar to most other Aegean plutons

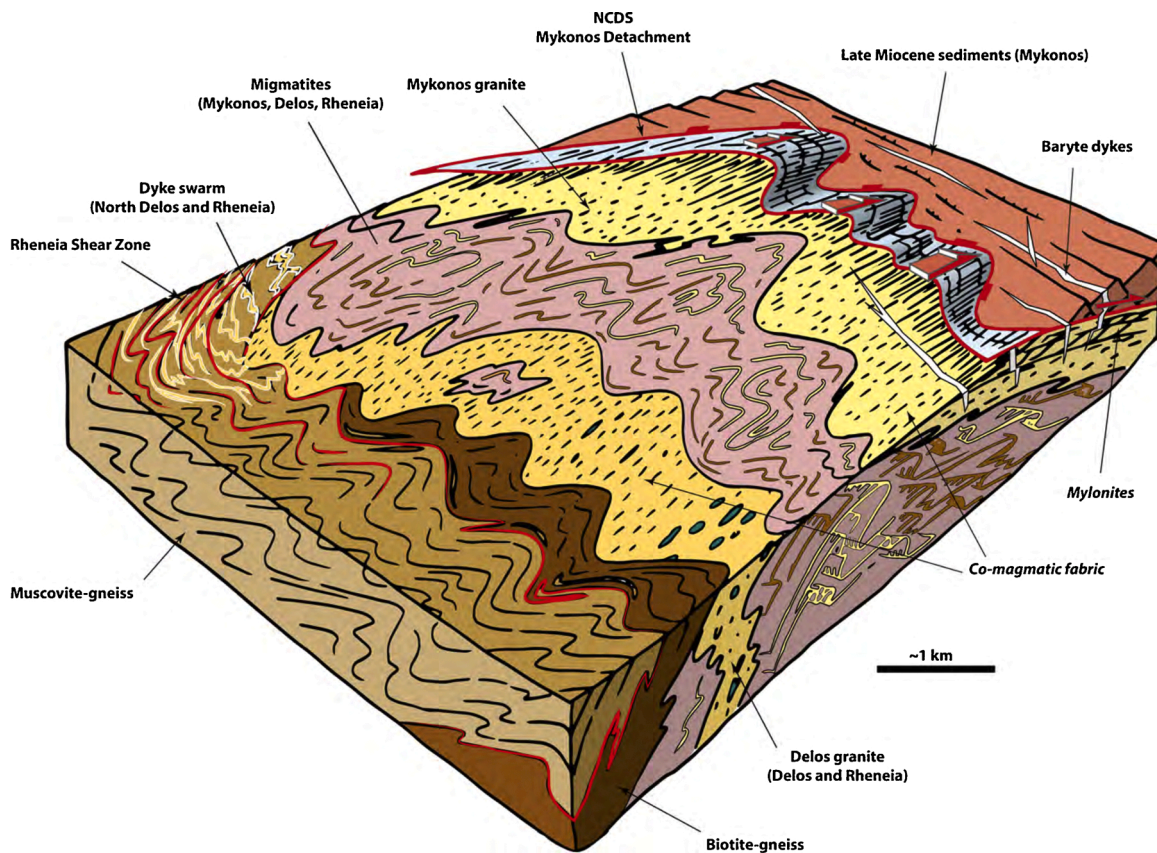


Fig. 14. Schematic 3-D diagram summarizing the observations on Delos and Rheneia.

as synthesized in Rabillard et al. (2017). A pluton rises within a ductile dome where the crust is partially molten and invades the dome below the NCDS (Figs. 9 & 11). The part of the pluton directly alimented locally by partial melting of the gneiss is unknown but probably quite significant when considering the gradual transition between the pluton and the migmatitic gneiss observed on Mykonos (Fig. S1). The relative motion of the rising dome with respect to the hanging-wall of the detachment induces a top-to-the east shearing distributed within a large part of the laccolith, from co-magmatic deformation to sub-solidus mylonitization below the detachment. The opposite side of the dome is intensely deformed in ductile conditions by the thick Rheneia Shear Zone but the sense of shear is not ascertained, either synthetic of the top-to-the east shearing of the detachment or top-to-the west, conjugate of the detachment and accommodating the dome rise. The kinematic indicators we have observed however suggest a top-to-the east sense of shear and we shall consider this solution in the following. Whatever the structural level, from the deep migmatitic dome to the supra-detachment basin, the same direction of stretching and the same direction of fold axes are preserved. A component of constriction perpendicular to the stretching direction controls the formation of these folds, which style evolves from top to base, from open to tight folds, like in other MCC in the Aegean region, especially Naxos (e.g. Vanderhaeghe, 2004). These folds accommodate the same direction of shortening perpendicular to the main stretching direction all along the extension stage and exhumation history of the dome. In Mykonos, the contemporaneity of the formation of migmatites and the intrusion shows that partial melting and coeval folding are both young, dating from the Middle and Late Miocene, as shown by U-Pb ages on zircon and lower temperature methods (13–9 Ma; Brichau et al., 2008).

In both cases, MDR and Naxos, folds with vertical axial planes are tighter at depth than in the upper structures suggesting a more intense

constriction in the deep parts of the MCC. This constrictional component is expected in a-type domes formed with a component of strike-slip motion at the boundary of the system (Le Pourhiet et al., 2012). To explain the shorter wavelength of folds in the core of the MCC an alternative solution might be proposed. The observed folding affects alternating layers of variable competence and the rheological contrast is probably very small in the partially molten domains as seen above. The wavelength of folds depends upon the layers thickness and the viscosity contrast between layers. If this contrast is small the wavelength should be small and the folds thus tighter.

The observations made in this study in Rheneia and Delos show the deep parts of the dome and the interactions in hot and ductile conditions with the intrusion, conditions that are not met in other Aegean domes. Most other examples show the ductile deformation associated with the lower detachment and the co-magmatic deformation in the root zone of the pluton, but not the hot interactions between the migmatites and the intrusions. In all cases except Rheneia and Delos, the observations show a sharp intrusive contact between the intrusion and the dome or with upper crustal levels with evidence of contact metamorphism at the contact, as in Naxos or Tinos, showing that the visible part of the granitoid intruded a dome that had already cooled down (Jansen, 1977; Bröcker and Franz, 1994; Jolivet and Patriat, 1999). In Naxos, the presence of large septas of ductilely deformed migmatitic gneiss within the granodioritic pluton at short distance from the contact (Bessière et al., 2017) testifies for the same sort of interactions between the pluton and the dome at depth, but they are not preserved as on Delos and Rheneia. This same situation is observed on Mykonos with the intrusion of the granite in the Upper Cycladic Unit metabasite in the vicinity of the Livada Detachment (Jolivet et al., 2010; Lecomte et al., 2010). The only other case where the hot contact between the migmatite dome and the intrusion could be observed is Ikaria where the hot contact between the

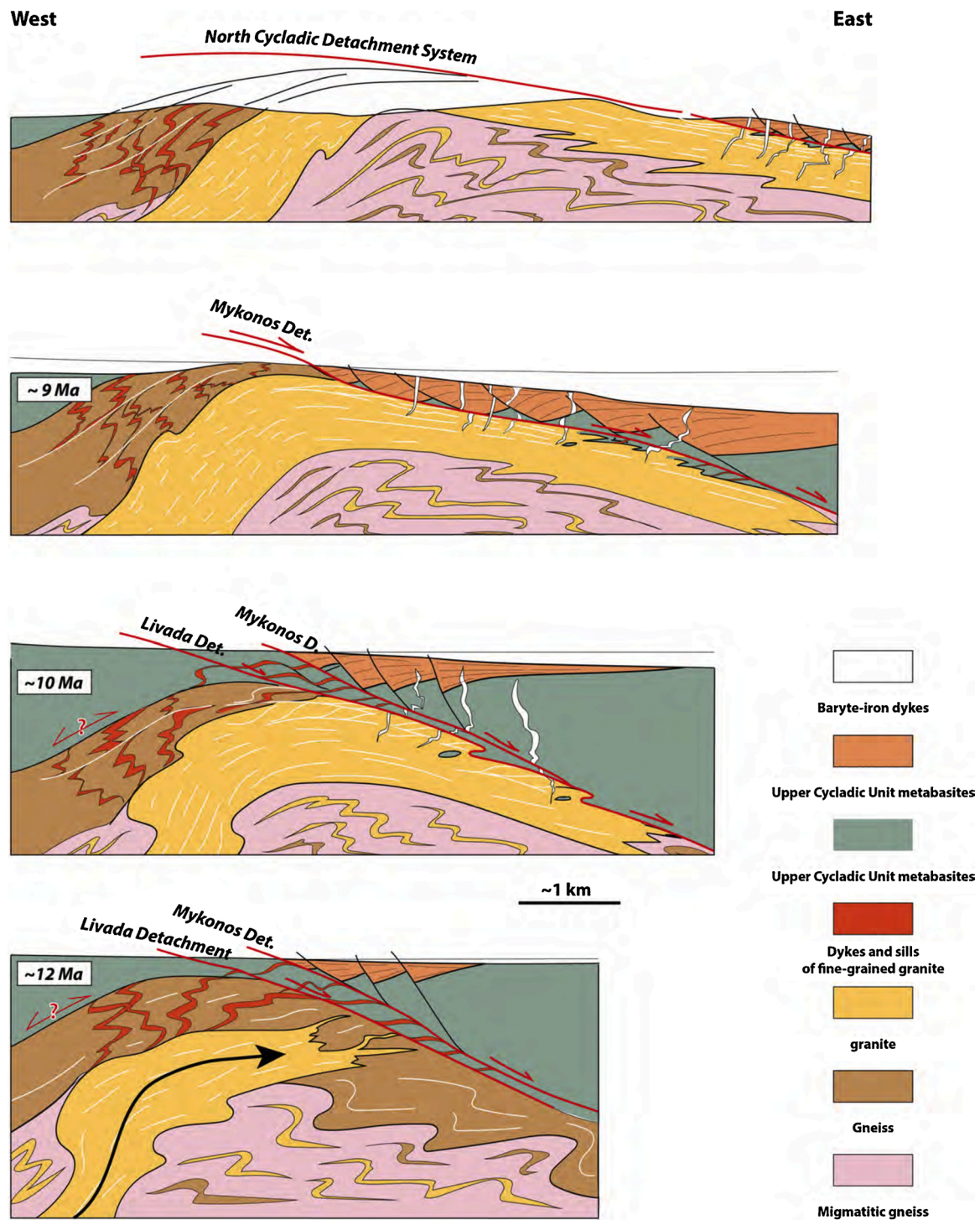


Fig. 15. Four stages of the progressive exhumation of the Mykonos-Delos-Rheneia metamorphic core complex from 12 Ma to the Present.

Karkinagrion leucogranite and the Miocene migmatite can be mapped but only in a restricted area (Beaudoin et al., 2015; Laurent et al., 2015). The case of Rheneia and Delos is thus a unique example in the Aegean to study the hot interactions between a rising pluton and its root zone within a migmatite dome because erosion reached much deeper levels of the MCC.

The contact zone observed on Delos between the granite and the migmatite shows a fuzzy transition with alternation of stromatic migmatites and granitic layers, both the migmatite and the granite being deformed with the same foliation and lineation direction. The flow

within the granite and the ductile deformation in the partially-molten gneiss are parallel, suggesting a very weak behavior of the gneiss when they are partially molten. *In-situ* melting of the gneiss is observed in the core of folds. Gneiss and marble enclaves of various size from a few cm to several hundred meters included within the granite show the same direction of stretching and the same foliation as the surrounding granite, also suggesting that the molten basement and the intrusion had similar rheologies at the time of inclusion. This observation is however not true everywhere as some sharp contacts between the gneiss with a preserved ductile deformation and the stretched granite show that the

interactions between the gneiss and the intrusion have lasted long enough to record a succession of magma batches during the same deformation event, the most recent ones arriving once the host rock was already cooler and thus more rigid. This is confirmed by the sharp contacts observed on Rheneia between the coarse granitic dykes near the main pluton and the biotite-gneiss, the host-rock and the dykes being intensely stretched along the regional X-direction. All these observations show a continuum of intrusion and coeval deformation during exhumation and cooling.

The Delos granite is intensely stretched and foliated in the central part in the vicinity of the sanctuary and south of it. The orientation of the feldspar megacrysts is parallel to the foliation in large migmatite enclaves and the transition from fuzzy diatexites to oriented granite with schlieren is progressive. This shows again that the rheologies of the molten gneiss and the pluton were not much different at the time of intrusion.

The significance of the biotite-gneiss and muscovite-gneiss must then be discussed. We observe a transition from gneiss intensely injected by dykes toward regularly laminated gneiss with alternation of leucocratic layers within the gneissic host rock, both in biotite- and muscovite gneiss. The most intense transposition is observed along the contact between these two types of gneiss and we interpret the transition as a thick shear zone, which we have named the *Rheneia Shear Zone*. One can then wonder how much of the layering observed in general in these gneiss, especially at a distance from the RSZ, is actually the result of the activity of the shear zone or an inheritance from an older deformation episode. Denèle et al. (2011) have interpreted the muscovite-gneiss of northern Rheneia as migmatitic. We do not follow this interpretation in this paper but it remains possible that the regular layering of these gneiss results from the recent shearing deformation of migmatitic gneiss, which would indicate a considerably thicker shear zone. Further field observations and sampling for dating with a range of radiochronological methods are required to answer this question.

The case-study of the MDR MCC thus shows a progressive transition from a weak dome where the intrusive granite has a rheology not much different from the partially molten host-rock to ultra-mylonites and brittle deformation along the main detachment. A continuum of deformation with E–W stretching and perpendicular shortening is observed from the ductile to the brittle stage. The intrusion of the granite within the dome is first associated with massive inclusion of ductile basement septas in the magma and progressive transitions between the granite and the migmatites are observed. While the whole system is exhumed and cools down, the granitic magma is emplaced within dykes of various scales while the same deformation continues. These dykes are observed all around the migmatite dome and the pluton and they intrude even the UCU at the top of the system. A thick shear zone forms above the dome, transposing the dykes. This lasts until the deformation localizes along a single detachment plane, the Mykonos Detachment and brittle formation of large Ba-Fe veins accompanies hydrothermal circulations during syn-kinematic cooling.

The duration of this progressive deformation is likely to be short. Observations show that the pluton and the migmatites are at least partly coeval. The age of the pluton is dated at 13 Ma using U-Pb on zircons on Mykonos and the brittle activity of the Mykonos Detachment between 13 and 9 Ma using mid- to low-temperature thermochronology (Brichau et al., 2008). The activity of the detachment, the formation of the Late Miocene Basin and the emplacement of the barite and iron-hydroxides ore lasted until ~9 Ma (Menant et al., 2013). 4 Myrs only thus separate the first intrusion from the end of extensional deformation along the NCDS. The age of the first extension in the Aegean started at ~30 Ma (Jolivet and Brun, 2010) or 21 Ma (Ring et al., 2010). Migmatites in the nearby Naxos-Paros dome has yielded ages as old as 20 Ma (Keay et al., 2001) but ages as young as 16 Ma have also been recovered on zircon rims (Martin et al., 2006) and late dykes cutting across the dome yielded even younger ages at ca. 13 Ma (Vanderhaeghe et al., 2018). More recent work by Ring et al. (2018) suggest that ages older than 18 Ma are

affected by some inheritance of older events and that the mean age for partial melting is about 14 Ma. On Ikaria the age of partial melting has been dated around 15–16 Ma (Beaudoin et al., 2015), similar to age of the oldest granitic pluton there (Bolhar et al., 2010). Partial melting in MDR thus probably started before the intrusion of the granite at 13 Ma but was still active at that time.

The pattern of stretching lineations (Figs. 3 and 10) seen across the MDR MCC shows a progressive rotation from E–W on Delos and Rheneia to NE–SW in the eastern part of Mykonos. This rotation had already been noticed by Denèle et al. (2011) who advocated for differential rotation during exhumation of the upper and lower portions of the crust. Paleomagnetic investigations in the Cyclades have indeed shown rotation about vertical axes of the plutonic bodies (Morris and Anderson, 1996; Avigad et al., 1998). The data suggest a clockwise rotation of the Mykonos pluton by about 22°. Avigad et al. (1998) used these evidence to suggest a decoupling between upper and lower crust during extension. The different orientation of stretching lineations in the northwest Cyclades (Tinos, Andros) and in the central Cyclades led Walcott and White (1998) to emphasize the importance of the so-called Mid-Cycladic Lineament, a complex strike-slip system that would separate two rigid blocks in the Cyclades. Le Pourhiet et al. (2012) show that a component of strike-slip distributed in the crust above a slab tear can explain the formation of a-type domes with their long axis parallel to the main direction of stretching and Jolivet et al. (2021) show that in such models the pattern of stretching lineations shows rotations in space compatible with the sense of this strike-slip motion. This change in stretching direction seen from Rheneia to eastern Mykonos should be reinterpreted in the framework of the slab tear that occurred underneath the eastern Aegean region between 15 and 8 Ma (Jolivet et al., 2015), including the full lineation map at the scale of the Cyclades and Western Anatolia.

8. Conclusion

The Mykonos-Delos-Rheneia MCC shows a unique example in the Aegean of the high-temperature interactions between a migmatitic dome intruded by a set of syn-kinematic intrusions in the footwall of a major low-angle detachment during a short period of a few Myrs. Compared to other MCC in the Cyclades, the MDR MCC better shows the deep parts of the dome where the intrusive rocks and the partially molten rocks of the dome have similar rheological parameters. The Naxos dome also shows a pluton intruding a migmatitic dome but the granodiorite is not seen in contact with the migmatitic core. The granodiorite intrusion instead pierces the outer parts of the dome. The MDR MCC thus allows describing the full evolution from the first intrusion of the pluton in the middle or lower crust to the extreme localization of deformation along a single detachment plane in the upper crust, all the way to the deposition of a supra-detachment basin invaded by hydrothermal venues during the last cooling steps. The whole extension process, from the ductile regime to the last brittle increment, was achieved with the same E–W stretching direction associated with E–W trending fold axes. The tightening of folds increase from the superficial one affecting the detachment to the deep ductile ones in the core of the migmatite dome. The intrusion starts at depth in hot conditions within the partially molten crust and the contact shows parallel flows in the granite and the migmatites indicating similar rheological behaviors between the deep molten crust and the intrusion. Large pieces of the molten gneiss and marbles are included in hot conditions within the pluton and the transition between the granite and the migmatite is often progressive. The exhumation of the dome was accompanied with the formation of a newly described thick shear zone enveloping the migmatitic core, the Rheneia Shear Zone. The presence of the shear zone is shown by the intense deformation of acidic dykes issued from the main granitic body and the core of the shear zone corresponds to the contact between the lower biotite-gneiss and the upper muscovite gneiss. The sense of shear is locally top-to-the east but additional observations are required to confirm this conclusion. The thickness of the

shear zone is also questionable as a part of the upper Rheneia gneiss could actually be part of the shear zone.

Author statement

Laurent Jolivet, Violaine Sautter, Isabelle Moretti, Tommy Vettor, Zozi Papadopoulou, Romain Augier and Laurent Arbaret did the field work, discussed the observations and wrote the manuscript. Yoann Denèle brought his past experience on Delos and Rheneia and discussed the content of the paper.

Declaration of Competing Interest

The authors report no declarations of interest.

Acknowledgments

This paper is a contribution of the ANR GAD project (ANR-18-CE27-0009-03). Special thanks are due to the Hellenic Ministry of Culture and Sports who allowed this project to be incorporated in the field survey of the Ephorate of Antiquities of the Cyclades of Rheneia and to the EFA (Ecole Française d'Athènes), in charge of the archeological survey on Delos who along with the Hellenic Ministry of Culture and Sports allowed us to study the island in the field and use the premises of the EFA on Delos during the field season. Thanks are also due to Armel Menant for his useful comments on an earlier version of this manuscript. Uwe Ring, Olivier Vanderhaeghe and Roger Buck reviewed this paper and their comments helped us preparing a more efficient manuscript.

Appendix A. Supplementary data

Supplementary material related to this article can be found, in the online version, at doi:<https://doi.org/10.1016/j.jog.2021.101824>.

References

- Altherr, R., Siebel, W., 2002. I-type plutonism in a continental back-arc setting: Miocene granitoids and monzonites from the central Aegean Sea, Greece. *Contrib. Mineral. Petrol.* 143, 397–415.
- Altherr, R., Kreuzer, H., Wendt, I., Lenz, H., Wagner, G.A., Keller, J., Harre, W., Hohndorf, A., 1982. A Late Oligocene/Early Miocene high temperature belt in the anti-cycladic crystalline complex (SE Pelagonian, Greece). *Geol. Jb.* 23, 97–164.
- Altherr, R., Henjes-Kunst, F., Matthews, A., Friedrichsen, H., Hansen, B.T., 1988. O-Sr isotopic variations in Miocene granitoids from the Aegean: evidence for an origin by combined assimilation and fractional crystallization. *Contrib. Mineral. Petrol.* 100, 528–541 doi:10.1007/BF00371381.
- Andriessen, P.A.M., Banga, G., Hebeda, E.H., 1987. Isotopic age study of pre-Alpine rocks in the basal units on Naxos, Sikinos and Ios, Greek Cyclades. *Geol. Mijnbouw* 66, 3–14.
- Aravadinou, E., Xypolias, P., Chatzaras, V., Iliopoulos, I., Gerogiannis, N., 2015. Ductile nappe stacking and refolding in the Cycladic Blueschist Unit: insights from Sifnos Island (south Aegean Sea). *Int. J. Earth Sci. (Geol. Rundsch.)*. DOI 10.1007/s00531-00015-01255-00532.
- Augier, R., Choulet, F., Faure, M., Turrillot, P., 2015a. A turning-point in the evolution of the Variscan orogen: the ca. 325 Ma regional partial-melting event of the coastal South Armorican domain (South Brittany and Vendée, France). *Bull. Soc. Géol. France* 186, 63–91. <https://doi.org/10.2113/gssgfbull.2186.2112-2113.2163>.
- Augier, R., Jolivet, L., Gadenne, L., Lahfid, A., Driussi, O., 2015b. Exhumation kinematics of the Cycladic Blueschists Unit and back-arc extension, insights from the Southern Cyclades (Sikinos and Folegandros Islands, Greece). *Tectonics* 34, 152–185. DOI: 10.1002/2014TC003664.
- Avdis, V., 2004. In: IGME (Ed.), *Geological Map of Greece, 1/50000, Mykonos-Rhinia Sheet*. Athens.
- Avigad, D., Matthews, A., Evans, B.W., Garfunkel, Z., 1992. Cooling during the exhumation of a blueschist terrane: sifnos (Cyclades, Greece). *Eur. J. Miner.* 4, 619–634.
- Avigad, D., Baer, G., Heimann, A., 1998. Block rotations and continental extension in the Central Aegean Sea: paleomagnetic and structural evidence from Tinos and Mykonos. *Earth Planet. Sci. Lett.* 157, 23–40. [https://doi.org/10.1016/S0012-1821X\(1098\)00024-00027](https://doi.org/10.1016/S0012-1821X(1098)00024-00027).
- Bargnesi, E.A., Stockli, D.F., Mancktelow, N., Soukis, K., 2013. Miocene core complex development and coeval supradetachment basin evolution of Paros, Greece, insights from (U–Th)/He thermochronometry. *Tectonophysics* 595–596, 165–182 doi.org/10.1016/j.tecto.2012.1007.1015.
- Beaudoin, A., Augier, R., Laurent, V., Jolivet, L., Lahfid, A., Bosse, V., Arbaret, L., Rabillard, A., Menant, A., 2015. The Ikaria high-temperature metamorphic core complex (cyclades, Greece): geometry, kinematics and thermal structure. *J. Geodyn.* 92, 18–41. <https://doi.org/10.1016/j.jog.2015.1009.1004>.
- Berthé, D., Choukroune, P., Jegouzo, P., 1979. Orthogneiss, mylonite and non coaxial deformation of granites : the example of the South Armorican Shear Zone. *J. Struct. Geol.* 1, 31–42.
- Bessière, E., Rabillard, A., Précigout, J., Arbaret, L., Jolivet, L., Augier, R., Menant, A., Mansard, N., 2017. Strain localization within a syn-tectonic intrusion in a back-arc extensional context: the Naxos monzogranite (Greece). *Tectonics* 37. <https://doi.org/10.1002/2017TC004801>.
- Biryol, C.B., Beck, S.L., Zandt, G., Özacar, A.A., 2011. Segmented African lithosphere beneath the Anatolian region inferred from teleseismic P-wave tomography. *Geophys. J. Int.* 184, 1037–1057 doi: 10.1111/j.1365-1246X.2010.04910.x.
- Blake, M.C., Bonneau, M., Geysant, J., Kienast, J.R., Lepvrier, C., Maluski, H., Papanikolaou, D., 1984. A geologic reconnaissance of the Cycladic blueschist belt, Greece: reply. *Geol. Soc. Am. Bull.* 95, 119–121.
- Bolhar, R., Ring, U., Allen, C.M., 2010. An integrated zircon geochronological and geochemical investigation into the Miocene plutonic evolution of the Cyclades, Aegean Sea, Greece: part 1: geochronology. *Contrib. Mineral. Petrol.* 160, 719–742. DOI 10.1007/s00410-00010-00504-00414.
- Bolhar, R., Ring, U., Kemp, A.L.S., Whitehouse, M.J., Weaver, S.D., Woodhead, J.D., Uysal, I.T., Turnbull, R., 2012. An integrated zircon geochronological and geochemical investigation into the Miocene plutonic evolution of the Cyclades, Aegean Sea, Greece: part 2: geochemistry. *Contrib. Mineral. Petrol.* 164, 915–933.
- Brichau, S., Ring, U., Ketcham, R.A., Carter, A., Stockli, D., Brunel, M., 2006. Constraining the long-term evolution of the slip rate for a major extensional fault system in the central Aegean, Greece, using thermochronology Earth and Pl. Sci. Lett. 241, 293–306 doi:10.1016/j.epsl.2005.1009.1065.
- Brichau, S., Ring, U., Carter, A., Monie, P., Bolhar, R., Stockli, D., Brunel, M., 2007. Extensional faulting on Tinos Island, Aegean Sea, Greece: how many detachments? *Tectonics* 26, TC4009 doi:10.1029/2006TC001969.
- Brichau, S., Ring, U., Carter, A., Bolhar, R., Monié, P., Stockli, D., Brunel, M., 2008. Timing, slip rate, displacement and cooling history of the Mykonos detachment footwall, Cyclades, Greece, and implications for the opening of the Aegean Sea basin. *J. Geol. Soc.* 165, 263–277 doi:10.1144/0016-76492006-76492145.
- Bröcker, M., Enders, M., 1999. U-Pb zircon geochronology of unusual eclogite-facies rocks from Syros and Tinos (Cyclades, Greece). *Geol. Mag.* 136, 111–118.
- Bröcker, M., Franz, L., 1994. The contact aureole on Tinos (Cyclades, Greece). Part I: field relationships, petrography and P-T conditions. *Chemie Der Erde - Geochem.* 54, 262–280.
- Brun, J.P., Faccenna, C., 2008. Exhumation of high-pressure rocks driven by slab rollback. *Earth Planet. Sci. Lett.* 272, 1–7. <https://doi.org/10.1016/j.epsl.2008.1002.1038>.
- Buick, I.S., 1991. Mylonite fabric development on Naxos, Greece. *J. Struct. Geol.* 13, 643–655.
- Buick, I.S., Holland, T.J.B., 1989. The P-T-t path associated with crustal extension, naxos, cyclades, Greece. In: Daly, J.S. (Ed.), *Evolution of Metamorphic Belts*, pp. 365–369 doi:10.1144/GSL.SP.1989.1043.1101.1132.
- Caggiannelli, A., Prosser, G., Rottura, A., 2000. Thermal history vs. Fabric anisotropy in granitoids emplaced at different crustal levels: an example from Calabria, southern Italy. *Terra Nova* 12, 109–116.
- Cayeux, L., 1911. *Exploration Archéologique De Délos*. Fontemoing et Cie, Paris.
- Charles, N., Gumiaux, C., Augier, R., Chen, Y., Zhu, R., Lin, W., 2011. Metamorphic Core Complexes vs. Synkinematic plutons in continental extension setting: insights from key structures (Shandong Province, eastern China). *J. Asian Earth Sci.* 40, 261–278 doi:10.1016/j.jseas.2010.1007.1006.
- de Boorder, H., Spakman, W., White, S.H., Wortel, M.J.R., 1998. Late Cenozoic mineralization, orogenic collapse and slab detachment in the European Alpine Belt. *Earth Planet. Sci. Lett.* 164, 569–575.
- de Saint Blanquat, M., Horsman, M.E., Habert, G., Morgan, S., Vanderhaeghe, O., Law, R., Tikoff, B., 2011. Multiscale magmatic cyclicality, duration of pluton construction, and the paradoxical relationship between tectonism and plutonism in continental arcs. *Tectonophysics* 500, 20–33 doi:10.1016/j.tecto.2009.2012.2009.
- de Saint-Blanquat, M., Law, R.D., Bouchez, J.L., Morgan, S.S., 2001. Internal structure and emplacement of the Papoose Flat pluton: an integrated structural, petrographic, and magnetic susceptibility study. *GSA Bull.* 113, 976–995.
- Denèle, Y., Lecomte, E., Jolivet, L., Lacombe, O., Labrousse, L., Huet, B., Le Pourhiet, L., 2011. Granite intrusion in a metamorphic core complex: the example of the Mykonos laccolith (Cyclades, Greece). *Tectonophysics* 501, 52–70. <https://doi.org/10.1016/j.tecto.2011.1001.1013>.
- Dercourt, J., Zonenshain, L.P., Ricou, L.E., Kuzmin, V.G., Le Pichon, X., Knipper, A.L., Grandjacquet, C., Sbertshikov, I.M., Geysant, J., Lepvrier, C., Pechevsky, D.H., Boulin, J., Sibuet, J.C., Savostin, L.A., Sorokhtin, O., Westphal, M., Bazhenov, M.L., Lauer, J.P., Biju-Duval, B., 1986. Geological evolution of the Tethys belt from the Atlantic to the Pamir since the Lias. *Tectonophysics* 123, 241–315.
- Desruelles, S., Fouache, E., 2007. Sea-level changes and shoreline reconstruction in the ancient city of Delos (Cyclades, Greece). *Geodin. Acta* 20, 231–239.
- Desruelles, S., Fouache, E., Attila Ciner, A., Dalongeville, R., Pavlopoulos, K., Kosun, E., Coquinot, Y., Potdevin, J.L., 2009. Beachrocks and sea level changes since Middle Holocene: comparison between the insular group of Mykonos-delos-rheneia (Cyclades, Greece) and the southern coast of Turkey. *Glob. Planet. Change* 66, 19–33. <https://doi.org/10.1016/j.gloplacha.2008.1007.1009>.
- Duchêne, S., Aïssa, R., Vanderhaeghe, O., 2006. Pressure-Temperature-time Evolution of Metamorphic Rocks from Naxos (Cyclades, Greece): constraints from Thermobarometry and Rb/Sr dating. *Geodyn. Acta* 19, 299–319.

- Ducoux, M., Branquet, Y., Jolivet, L., Arbaret, L., Grasemann, B., Rabillard, A., Gumiaux, C., Drufin, S., 2016. Synkinematic skarns and fluid drainage along detachments: the West Cycladic Detachment System on Serifos Island (Cyclades, Greece) and its related mineralization. *Tectonophysics* 695, 1–26 <https://doi.org/10.1016/j.tecto.2016.1012.1008>.
- Faure, M., Bonneau, M., 1988. Données nouvelles sur l'extension néogène de l'Égée: la déformation ductile du granite miocène de Mykonos (Cyclades, Grèce). *C. R. Acad. Sci. Paris* 307, 1553–1559.
- Faure, M., Bonneau, M., Pons, J., 1991. Ductile deformation and syntectonic granite emplacement during the late Miocene extension of the Aegean (Greece). *Bull. Soc. géol. France* 162, 3–12.
- Gapais, D., Lagarde, J.L., Lecorre, C., Audren, C., Jégouzo, P., Casas Sainz, A., Van Den Driessche, J., 1993. The Quiberon Shear Zone - evidence for carboniferous extension in the Variscan Belt of South Brittany (France). *C. R. Acad. Sci. Paris* 316, 1123–1129.
- Gautier, P., Brun, J.P., 1994a. Crustal-scale geometry and kinematics of late-orogenic extension in the central Aegean (Cyclades and Evvia island). *Tectonophysics* 238, 399–424 [doi:10.1016/0040-1951\(1994\)90066-90063](https://doi.org/10.1016/0040-1951(1994)90066-90063).
- Gautier, P., Brun, J.P., 1994b. Ductile crust exhumation and extensional detachments in the central Aegean (Cyclades and Evvia islands). *Geodin. Acta* 7, 57–85.
- Gautier, P., Brun, J.P., Jolivet, L., 1993. Structure and kinematics of upper Cenozoic extensional detachment on Naxos and Paros (Cyclades Islands, Greece). *Tectonics* 12, 1180–1194 [doi:10.1029/1993TC001131](https://doi.org/10.1029/1993TC001131).
- Gautier, P., Brun, J.P., Moriceau, R., Sokoutis, D., Martinod, J., Jolivet, L., 1999. Timing, kinematics and cause of Aegean extension: a scenario based on a comparison with simple analogue experiments. *Tectonophysics* 315, 31–72.
- Grasemann, B., Petrakakis, K., 2007. Evolution of the serifos metamorphic core complex. *J. Virtual Explor.* 27, 1–18.
- Grasemann, B., Schneider, D.A., Stockli, D.F., Iglseder, C., 2012. Miocene divergent crustal extension in the Aegean: evidence from the western Cyclades (Greece). *Lithosphere*. <https://doi.org/10.1130/L1164.1131>.
- Grasemann, B., Huet, B., Schneider, D.A., Rice, H.N., Lemonnier, N., Tschegg, C., 2017. Miocene postorogenic extension of the Eocene synorogenic imbricated Hellenic subduction channel: new constraints from Milos (Cyclades, Greece). *GSA Bull.* <https://doi.org/10.1130/B31731.31731>.
- Groppo, C., Forster, M., Lister, G., Compagnoni, R., 2009. Glaucofane schists and associated rocks from Sifnos (Cyclades, Greece): new constraints on the P–t evolution from oxidized systems. *Lithos* 109, 254–273 [doi:10.1016/j.lithos.2008.10.1005](https://doi.org/10.1016/j.lithos.2008.10.1005).
- Hetzl, R., Passchier, C.W., Ring, U., Dora, O.O., 1995a. Bivergent extension in orogenic belts: the Menderes massif (southwestern Turkey). *Geology* 23, 455–458.
- Hetzl, R., Ring, U., Akal, A., Troesch, M., 1995b. Miocene NNE-directed extensional unroofing in the Menderes massif, southwestern Turkey. *J. Geol. Soc. London* 152, 639–654. <https://doi.org/10.1144/gsjgs.152.4.0639>.
- Holm, D.K., 1995. Relation of deformation and multiple intrusion in the Death Valley extended region, California, with implications for magma entrapment mechanism. *J. Geophys. Res.* 100 (10), 495–410,505.
- Huet, B., Labrousse, L., Jolivet, L., 2009. Thrust or detachment? Exhumation processes in the Aegean: insight from a field study on Ios (Cyclades, Greece). *Tectonics* 28, TC3007 [doi:10.1029/2008TC002397](https://doi.org/10.1029/2008TC002397).
- Huet, B., Le Pourhiet, L., Labrousse, L., Burov, E., Jolivet, L., 2011. Formation of metamorphic core complex in inherited wedges: a thermomechanical modelling study. *Earth Planet. Sci. Lett.* <https://doi.org/10.1016/j.epsl.2011.07.004>.
- Hutton, D.H.W., 1988. Granite emplacement mechanisms and tectonic controls: inferences from deformation studies. *Trans. R. Soc. Edinb. Earth Sci.* 79, 245–255.
- Hutton, D.H.W., Dempster, T.J., Brown, P.E., Becker, S.D., 1990. A new mechanism of granite emplacement: intrusion in active extensional shear zones. *Nature* 343, 452–455.
- Iglseder, C., Grasemann, B., Rice, A.H.N., Petrakakis, K., Schneider, D.A., 2011. Miocene south directed low-angle normal fault evolution on Kea (West Cycladic Detachment System, Greece). *Tectonics* 30, TC4013 [doi:10.1029/2010TC002802](https://doi.org/10.1029/2010TC002802).
- Jansen, J.B.H., 1977. Metamorphism on Naxos. Utrecht University, Greece.
- Ji, W., Faure, M., Lin, W., Chen, Y., Chu, Y., Xue, Z., 2018. Multiple emplacement and exhumation history of the Late Mesozoic Dayunshan–mufushan batho-lith in southeast China and its tectonic significance: 1. Structural analysis and geochronological constraints. *J. Geophys. Res. Solid Earth* 123, 689–710 <https://doi.org/10.1002/2017JB014597>.
- Jolivet, L., Brun, J.P., 2010. Cenozoic geodynamic evolution of the Aegean region. *Int. J. Earth Sci.* 99, 109–138. DOI: 110.1007/s00531-00008-00366-00534.
- Jolivet, L., Patriat, M., 1999. Ductile extension and the formation of the aegean Sea. In: Durand, B., Jolivet, L., Horváth, F., Séranne, M. (Eds.), *The Mediterranean Basins: Tertiary Extension Within the Alpine Orogen*. Geological Society, London, pp. 427–456 [doi:10.1144/GSL.SP.1999.1156.1101.1120](https://doi.org/10.1144/GSL.SP.1999.1156.1101.1120).
- Jolivet, L., Brun, J.P., Gautier, P., Lallemand, S., Patriat, M., 1994a. 3-D kinematics of extension in the Aegean from the Early Miocene to the Present, insight from the ductile crust. *Bull. Soc. géol. France* 165, 195–209.
- Jolivet, L., Daniel, J.M., Truffert, C., Goffé, B., 1994b. Exhumation of deep crustal metamorphic rocks and crustal extension in back-arc regions. *Lithos* 33, 3–30. [https://doi.org/10.1016/0024-4937\(1994\)90051-90055](https://doi.org/10.1016/0024-4937(1994)90051-90055).
- Jolivet, L., Famin, V., Mehl, C., Parra, T., Aubourg, C., Hébert, R., Philippot, P., 2004a. Strain localization during crustal-scale bounding to form extensional metamorphic domes in the Aegean Sea. In: Whitney, D.L., Teyssier, C., Siddoway, C.S. (Eds.), *Gneiss Domes in Orogeny*. Geological Society of America, Boulder, Colorado, pp. 185–210.
- Jolivet, L., Rimmelé, G., Oberhänsli, R., Goffé, B., Candan, O., 2004b. Correlation of syn-orogenic tectonic and metamorphic events in the Cyclades, the Lycian Nappes and the Menderes massif, geodynamic implications. *Bull. Geol. Soc. France* 175, 217–238 [doi:10.2113/2175.2113.2217](https://doi.org/10.2113/2175.2113.2217).
- Jolivet, L., Goffé, B., Monié, P., Truffert-Luxey, C., Patriat, M., Bonneau, M., 1996. Miocene detachment in Crete and exhumation P–T–t paths of high pressure metamorphic rocks. *Tectonics* 15, 1129–1153.
- Jolivet, L., Lecomte, E., Huet, B., Denèle, Y., Lacombe, O., Labrousse, L., Le Pourhiet, L., Mehl, C., 2010. The north cycladic detachment system. *Earth Planet. Sci. Lett.* 289, 87–104 [doi:10.1016/j.epsl.2009.10.1032](https://doi.org/10.1016/j.epsl.2009.10.1032).
- Jolivet, L., Faccenna, C., Huet, B., Labrousse, L., Le Pourhiet, L., Lacombe, O., Lecomte, E., Burov, E., Denèle, Y., Brun, J.P., Philippon, M., Paul, A., Salaün, G., Karabulut, H., Piromallo, C., Monié, P., Gueydan, F., Okay, A.I., Oberhänsli, R., Pourteau, A., Augier, R., Gadenne, L., Driussi, O., 2013. Aegean tectonics: strain localisation, slab tearing and trench retreat. *Tectonophysics* 597–598. <https://doi.org/10.1016/j.tecto.2012.06.011>, 1–33.
- Jolivet, L., Menant, A., Sternal, P., Rabillard, A., Arbaret, L., Augier, R., Laurent, V., Beaudoin, A., Grasemann, B., Huet, B., Labrousse, L., Le Pourhiet, L., 2015. The geological signature of a slab tear below the Aegean. *Tectonophysics* 659 (166–182), 166–182, [doi:10.1016/j.tecto.2015.1008.1004](https://doi.org/10.1016/j.tecto.2015.1008.1004).
- Jolivet, L., Menant, A., Roche, V., Le Pourhiet, L., Maillard, A., Augier, R., Do Couto, D., Gorini, C., Thion, I., Canva, A., 2021. Transfer Zones in Mediterranean Back-arc Regions and Tear Faults. *BSGF-Earth Sciences Bulletin* in press.
- Katzir, Y., Matthews, A., Garfunkel, Z., Schliestedt, M., Avigad, D., 1996. The tectono-metamorphic evolution of a dismembered ophiolite (Tinos, Cyclades, Greece). *Geol. Mag.* 133, 237–254.
- Keay, S., Lister, G., Buick, I., 2001. The timing of partial melting, Barrovian metamorphism and granite intrusion in the Naxos metamorphic core complex, Cyclades, Aegean Sea, Greece. *Tectonophysics* 342, 275–312 [doi:10.1016/S0040-1951\(1001\)00168-00168](https://doi.org/10.1016/S0040-1951(1001)00168-00168).
- Keiter, M., Piepjohn, K., Ballhaus, C., Lagos, M., Bode, M., 2004. Structural development of high-pressure metamorphic rocks on Syros island (Cyclades, Greece). *J. Struct. Geol.* 26, 1433–1445 [doi:10.1016/j.jsg.2003.14.11027](https://doi.org/10.1016/j.jsg.2003.14.11027).
- Kruckenberger, S.C., Vanderhaeghe, O., Ferré, E.C., Teyssier, C., Whitney, D.L., 2011. Flow of partially molten crust and the internal dynamics of a migmatite dome, Naxos, Greece: internal dynamics of the Naxos dome. *Tectonics* 30, 1–24. <https://doi.org/10.1029/2010TC002751>.
- Labrousse, L., Huet, B., Le Pourhiet, L., Jolivet, L., Burov, E., 2016. Rheological implications of extensional detachments: mediterranean and numerical insights. *Earth. Rev.* 161, 233–258 <https://doi.org/10.1016/j.earscirev.2016.1009.1003>.
- Lamont, T.N., Searle, M.P., Waters, D.J., Roberts, N.M.W., Palin, R.M., Smye, A., Dyck, B., Gopon, P., Weller, O.M., St-Onge, M.R., 2018. Compressional origin of the Naxos metamorphic core complex, Greece: structure, petrography, and thermobarometry. *GSA Bull.* <https://doi.org/10.1130/B31978.31971>.
- Lamont, T.N., Roberts, N.M.W., Searle, M.P., Gopon, P., Waters, D.J., Millar, I., 2020. The age, origin, and emplacement of the Tsiknias Ophiolite, Tinos, Greece. *Tectonics* 39 e2019TC00567; <https://doi.org/10.1029/2019TC005677>.
- Laurent, V., Beaudoin, A., Jolivet, L., Arbaret, L., Augier, R., Rabillard, A., 2015. Interrelations between extensional shear zones and synkinematic intrusions: the example of Ikaria Island (NE Cyclades, Greece). *Tectonophysics* 651–652, 152–171 <https://doi.org/10.1016/j.tecto.2015.1003.1020>.
- Laurent, V., Jolivet, L., Roche, V., Augier, R., Scaillet, S., Cardello, L., 2016. Strain localization in a fossilized subduction channel: insights from the Cycladic Blueschist Unit (Syros, Greece). *Tectonophysics* 672–673, 150–169 <https://doi.org/10.1016/j.tecto.2016.1001.1036>.
- Laurent, V., Huet, B., Labrousse, L., Jolivet, L., Monié, P., Augier, R., 2017. Extraneous argon in high-pressure metamorphic rocks: distribution, origin and transport in the Cycladic Blueschist Unit (Greece). *Lithos* 272–273, 315–335 <https://doi.org/10.1016/j.lithos.2016.1012.1013>.
- Le Pichon, X., Angelier, J., 1979. The Hellenic arc and trench system: a key to the neotectonic evolution of the eastern Mediterranean area. *Tectonophysics* 60, 1–42.
- Le Pichon, X., Angelier, J., 1981a. The Aegean Sea. *Phil. Trans. Roy. Soc. London* 300, 357–372.
- Le Pichon, X., Angelier, J., 1981b. The Hellenic arc and trench system: a key to the neotectonic evolution of the eastern mediterranean area. *Phil. Trans., R. Soc. London* 300, 357–372.
- Le Pourhiet, L., Burov, E., Moretti, I., 2004. Rifting through a stack of inhomogeneous thrusts (the dipping pie concept). *Tectonics* 23. <https://doi.org/10.1029/2003TC001584>.
- Le Pourhiet, L., Huet, B., May, D.A., Labrousse, L., Jolivet, L., 2012. Kinematic interpretation of the 3D shapes of metamorphic core complex. *Geochem. Geophys. Geosyst.* 13, Q09002 [doi:10.1029/2012GC004271](https://doi.org/10.1029/2012GC004271).
- Lecomte, E., Jolivet, L., Lacombe, O., Denèle, Y., Labrousse, L., Le Pourhiet, L., 2010. Geometry and kinematics of a low-angle normal fault on Mykonos island (Cyclades, Greece): evidence for slip at shallow dip. *Tectonics* 29, TC5012 [doi:10.1029/2009TC002564](https://doi.org/10.1029/2009TC002564).
- Lee, J., Lister, G.S., 1992. Late Miocene ductile extension and detachment faulting, Mykonos, Greece. *Geol.* 20, 121–124 [doi:10.1130/0091-7613\(1992\)1020<0121:L MDEAD>1132.CO;1](https://doi.org/10.1130/0091-7613(1992)1020<0121:L MDEAD>1132.CO;1).
- Liati, A., Skarpelis, N., Pe-Piper, G., 2009. Late Miocene magmatic activity in the Attic-Cycladic Belt of the Aegean (Lavrion, SE Attica, Greece): implications for the geodynamic evolution and timing of ore deposition. *Geol. Mag.* 146, 732–742 [doi:10.1017/S0016756809006438](https://doi.org/10.1017/S0016756809006438).
- Lin, W., Charles, N., Chen, Y., Chen, K., Faure, M., Wu, L., Wang, F., Li, Q., Wang, J., Wang, Q., 2013. Late Mesozoic compressional to extensional tectonics in the Yiwulushan massif, NE China and their bearing on the Yinshan-Yanshan orogenic belt Part II: Anisotropy of magnetic susceptibility and gravity modeling. *Gondwana Res.* 23, 78–94.

- Lister, G.S., Raouzaoui, A., 1996. The tectonic significance of a porphyroblastic blueschist facies overprint during Alpine orogenesis: sifnos, Aegean Sea, Greece. *J. Struct. Geol.* 18, 1417–1436.
- Lister, G.S., Banga, G., Feenstra, A., 1984. Metamorphic core complexes of cordilleran type in the Cyclades, Aegean Sea, Greece. *Geol.* 12, 221–225 doi:210.1130/0091-7613(1984)1112<1221:MC COCT>1132.1130.CO;1132.
- Lucas, L., 1999. Le Pluton De Mykonos-delos-Rhenee (Cyclades, Grèce): Un Exemple De Mise En Place Synchrone De l'extension Crustale. Université d'Orléans, Orléans, p. 491.
- Maluski, H., Bonneau, M., Kienast, J.R., 1987. Dating the metamorphic events in the Cycladic area: 39Ar/40Ar data from metamorphic rocks of the island of Syros (Greece). *Bull. géol. Soc. France* 8, 833–842.
- Martha, S.O., Dörr, W., Gerdes, A., Petschick, R., Schastok, J., Xypolias, P., Zulauf, G., 2016. New structural and U–Pb zircon data from Anafi crystalline basement (Cyclades, Greece): constraints on the evolution of a Late Cretaceous magmatic arc in the Internal Hellenides. *Int. J. Earth Sci.* 105, 2031–2060 doi:210.1007/s00531-00016-01346-00538.
- Martin, L., Duchêne, S., Deloule, E., Vanderhaeghe, O., 2006. The isotopic composition of zircon and garnet: a record of the metamorphic history of Naxos, Greece. *Lithos* 87, 174–192 doi:110.1016/j.lithos.2005.1006.1016.
- Maxeiner, R.O., Ashton, K., Card, C.D., Morelli, R.M., Knox, B., 2017. A Field Guide to Naming Migmatites and Their Textures, With Saskatchewan Examples, Summary of Investigations, Miscellaneous Report 2017-4.2, Paper A-2. Saskatchewan Geological Survey. Saskatchewan Ministry of the Economy, p. 21.
- Menant, A., Jolivet, L., Augier, R., Skarpelis, N., 2013. The North Cycladic Detachment System and associated mineralization, Mykonos, Greece: insights on the evolution of the Aegean domain. *Tectonics* 32, 433–452 doi:410.1002/tect.20037.
- Menant, A., Jolivet, L., Vrielynck, B., 2016. Kinematic reconstructions and magmatic evolution illuminating crustal and mantle dynamics of the eastern Mediterranean region since the late Cretaceous. *Tectonophysics* 675, 103–140 doi: 110.1016/j.tecto.2016.1003.1007.
- Mizera, M., Behrmann, J.H., 2015. Strain and flow in the metamorphic core complex of Ios Island (Cyclades, Greece). *Int. J. Earth Sci. (Geol. Rundsch.)* https://doi.org/10.1007/s00531-00015-01259-y.
- Morris, A., Anderson, A., 1996. First paleomagnetic results from the Cycladic Massif, Greece, and their implications for Miocene extension directions and tectonic models in the Aegean. *Earth Planet. Sci. Lett.* 142, 397–408.
- Papanikolaou, D.J., 1979. Contribution to the geology of the Aegean Sea: the island of Paros. *Ann. Géol. Pays Hellén.* 30, 65–96.
- Paterson, S.R., Tobisch, O.T., 1992. Rates of processes in magmatic arcs: implications for the timing and nature of pluton emplacement and wall rock deformation. *J. Struct. Geol.* 14, 291–300.
- Pe-Piper, G., Piper, D.J.W., 2006. Unique features of the Cenozoic igneous rocks of Greece. In: Dilek, Y., Pavlides, S. (Eds.), *Postcollisional Tectonics and Magmatism in the Mediterranean Region and Asia*. Geological Society of America Special Paper, 409 Geological Society of America, pp. 259–282 doi: 210.1130/2006.2409(1114).
- Pe-Piper, G., Piper, D.J.W., Matarangas, D., 2002. Regional implications of geochemistry and style of emplacement of Miocene I-type diorite and granite, Delos, Cyclades, Greece. *Lithos* 60, 47–66. https://doi.org/10.1016/S0024-4937(1001)00068-00068.
- Philippou, M., Brun, J.P., Gueydan, F., 2011. Tectonics of syros island blueschists (Cyclades, Greece): from subduction to Aegean extension. *Tectonics* 30, TC4001 doi: 4010.1029/2010TC002810.
- Poulaki, E.M., Stockli, D.F., Flansburg, M.E., Soukis, K., 2019. Zircon U–Pb chronostratigraphy and provenance of the cycladic blueschist unit and the nature of the contact with the cycladic basement on Sikinos and Ios Islands, Greece. *Tectonics* 38, 3586–3613 https://doi.org/3510.1029/2018TC005403.
- Rabillard, A., Arbaret, L., Jolivet, L., Le Breton, N., Gumiaux, C., Augier, R., Grasmann, B., 2015. Interactions between plutonism and detachments during metamorphic core complex formation, Serifos Island (Cyclades, Greece). *Tectonics* 34, 1080–1106. DOI: 1010.1002/2014TC003650.
- Rabillard, A., Jolivet, L., Arbaret, L., Bessière, E., Laurent, V., Menant, A., Augier, R., Beaudoin, A., 2017. Interactions between plutonism and detachments: evidence from the Cyclades (Aegean Sea, Greece). *Tectonics* https://doi.org/10.1029/2017TC004697.
- Reinecke, T., Altherr, R., Hartung, B., Hatzipanagiotou, K., Kreuzer, H., Harre, W., Klein, H., Keller, J., Geenen, E., Böger, H., 1982. Remnants of a late Cretaceous high temperature belt on the island of Anafi (Cyclades, Greece). *N. Jb. Miner. Abh* 145, 157–182.
- Rice, H.N., Iglseider, C., Grasmann, B., Zamolyi, A., Nikolakopoulos, K.G., Mitropoulos, D., Voit, K., Müller, M., Draganits, E., Rockenschaub, M., Tsombos, P.I., 2012. A new geological map of the crustal-scale detachment on Kea (Western Cyclades, Greece). *Austrian J. Earth Sci.* 105, 108–124.
- Ricou, L.E., Burg, J.P., Godfriaux, L., Ivanov, Z., 1998. Rhodope and Vardar: the metamorphic and orostromic paired belts related to the Cretaceous subduction under Europe. *Geodin. Acta* 11, 285–309.
- Ring, U., Glodny, J., Will, T., Thomson, S., 2007. An Oligocene extrusion wedge of blueschists-facies nappes on Evia, Aegean Sea, Greece: implications for the early exhumation of high-pressure rocks. *J. Geol. Soc.* 164, 637–652 doi:610.1144/0016-76492006-76492041.
- Ring, U., Glodny, J., Will, T., Thomson, S., 2010. The Hellenic subduction system: high-pressure metamorphism, exhumation, normal faulting, and large-scale extension. *Annu. Rev. Earth Planet. Sci.* 38, 45–76. https://doi.org/10.1146/annurev.earth.050708.170910.
- Ring, U., Glodny, J., Will, T.M., Thomson, S., 2011. Normal faulting on Sifnos and the South Cycladic Detachment System, Aegean Sea, Greece. *J. Geol. Soc. Lond.* 168, 751–768 doi: 710.1144/0016-76492010-76492064.
- Ring, U., Glodny, J., Peillod, A., Skelton, A., 2018. The timing of high-temperature conditions and ductile shearing in the T footwall of the Naxos extensional fault system, Aegean Sea, Greece. *Tectonophysics* 745, 366–381 https://doi.org/310.1016/j.tecto.2018.1009.1001.
- Roche, V., Laurent, V., Cardello, G.L., Jolivet, L., Scaillet, S., 2016. The anatomy of the cycladic blueschist unit on sifnos island (Cyclades, Greece). *J. Geodyn.* 97, 62–87. https://doi.org/10.1016/j.jog.2016.1003.1008.
- Roche, V., Conand, C., Jolivet, L., Augier, R., 2018. Tectonic evolution of Leros (Dodecanese, Greece) and correlations between the Aegean Domain and the Menderes Massif. *J. Geol. Soc. Lond.* https://doi.org/10.1144/jgs2018-1028.
- Roche, V., Jolivet, L., Papanikolaou, D., Bozkurt, E., Menant, A., Rimmelé, G., 2019. Slab fragmentation beneath the Aegean/Anatolia transition zone: insights from the tectonic and metamorphic evolution of the Eastern Aegean region. *Tectonophysics* 754, 101–129 https://doi.org/110.1016/j.tecto.2019.1001.1016.
- Sanchez-Gomez, M., Avigad, D., Heiman, A., 2002. Geochronology of clasts in allochthonous Miocene sedimentary sequences on Mykonos and Paros islands: implications for back-arc extension in the Aegean Sea. *J. Geol. Soc.* 159, 45–60. https://doi.org/10.1144/0016-764901031.
- Sawyer, E.W., 2008. *Atlas of Migmatites*. NRC Research Press, Ottawa, Ontario, Canada.
- Sawyer, E.W., Brown, M., 2008. Working With Migmatites.
- Schmid, S.M., Bernoulli, D., Fügenschuh, B., Matenco, L., Schefer, S., Schuster, R., Tischler, M., Ustaszewski, K., 2008. The Alpine-Carpathian-Dinaric orogenic system: correlation and evolution of tectonic units. *Swiss J. Geosci.* 101, 139–183. DOI 110.1007/s00015-00008-01247-00013.
- Schneider, D.A., Soukis, K., Grasmann, B., Draganits, E., 2018. Geodynamic significance of the santorini detachment system (Cyclades, Greece). *Terra Nova* 30, 414–422. DOI: 410.1111/ter.12357.
- Schumacher, J.C., Brady, J.B., Cheney, J.T., Tonnsen, R.R., 2008. Glaucofane-bearing marbles on syros, Greece. *J. Petrol.* 49, 1667–1686 doi:1610.1093/petrology/egn1042.
- Shaked, Y., Avigad, D., Garfunkel, Z., 2000. Alpine high-pressure metamorphism of the Almyropotamos window (southern Evia, Greece). *Geol. Mag.* 137, 367–380.
- Simaiakis, S.M., Rijdsdijk, K.F., Koene, E.F.M., Norder, S.J., Van Boxel, J.H., Stocchi, P., Hammoud, C., Kougioumoutzis, K., Georgopoulou, E., Van Lon, E., Tjørve, K.M.C., Tjørve, E., 2017. Geographic changes in the Aegean Sea since the Last Glacial Maximum: postulating biogeographic effects of sea-level rise on islands. *Palaeogeogr. Palaeoclimatol. Palaeoecol.* 471, 108–119 https://doi.org/110.1016/j.palaeo.2017.1002.1002.
- Skarpelis, N., Kyriakopoulos, K., Villa, I., 1992. Occurrence and 40Ar/39Ar dating of a granite in Thera (santorini, Greece). *Geol. Rundschau* 81, 729–735.
- Soukis, K., Stöckli, D., 2013. Structural and thermochronometric evidence for multi-stage exhumation of Southern Syros, Cycladic Islands, Greece. *Tectonophysics* 595–596, 148–164 doi:110.1016/j.tecto.2012.1005.1017.
- Stouraiti, C., Mitropoulos, P., Tarney, J., Barreiro, B., McGrath, A.M., Baltatzis, E., 2010. Geochemistry and petrogenesis of late Miocene granitoids, Cyclades, southern Aegean: nature of source components. *Lithos* 114, 337–352 doi:310.1016/j.lithos.2009.1009.1010.
- Strecker, A., 1975. To each plutonic rock its proper name. *Earth-Sci. Rev.* 12, 1–33.
- Tombros, S.F., St. Seymour, K., Williams-Jones, A.E., Zhai, D., Liu, J., 2015. Origin of a barite-sulfide ore deposit in the Mykonos intrusion, cyclades: Trace element, isotopic, fluid inclusion and raman spectroscopy evidence. *Ore Geol. Rev.* 67, 139–157 https://doi.org/110.1016/j.oregeorev.2014.1011.1016.
- Tremblay, A., Meshi, A., Deschamps, T., Goulet, F., Goulet, N., 2015. The Vardar zone as a suture for the Mirdita ophiolites, Albania: constraints from the structural analysis of the Korabi-Pelagonian zone. *Tectonics* 34, 352–375 doi:310.1002/2014TC003807.
- Trotet, F., Jolivet, L., Vidal, O., 2001a. Tectono-metamorphic evolution of Syros and Sifnos islands (Cyclades, Greece). *Tectonophysics* 338, 179–206.
- Trotet, F., Vidal, O., Jolivet, L., 2001b. Exhumation of Syros and Sifnos metamorphic rocks (Cyclades, Greece). New constraints on the P–T paths. *Eur. J. Mineral.* 13, 901–920 doi:910.1127/0935-1221/2001/0013/0901.
- Tschegg, C., Grasmann, B., 2009. Deformation and alteration of a granodiorite during low-angle normal faulting (Serifos, Greece). *Lithosphere* 1, 139–154. https://doi.org/10.1130/L33.1.
- Urai, J.L., Shuiling, R.D., Jansen, J.B.H., 1990. Alpine deformation on naxos (Greece). In: Knipe, R.J., Rutter, E.H. (Eds.), *Deformation Mechanisms, Rheology and Tectonics*. *Geol. Soc. spec. Pub.*, pp. 509–522 doi:510.1144/GSL.SP.1990.1054.1101.1147.
- van Hinsbergen, D.J.J., Langereis, C.G., Meulenkamp, J.E., 2005. Revision of the timing, magnitude and distribution of Neogene rotations in the western Aegean region. *Tectonophysics* 396, 1–34.
- Vandenbergh, L.C., Lister, G.S., 1996. Structural analysis of basement tectonics from the Aegean metamorphic core complex of Ios, Cyclades, Greece. *J. Struct. Geol.* 18, 1437–1454 doi:1410.1016/S0191-8141(1496)00068-.
- Vanderhaeghe, O., 2001. Melt segregation, pervasive melt migration and magma mobility in the continental crust: the structural record from pores to Orogens. *Phys. Chem. Earth* 26, 213–223.
- Vanderhaeghe, O., 2004. Structural development of the naxos migmatite dome. In: Whitney, D.L., Teyssier, C., Siddoway, C.S. (Eds.), *Gneiss Domes in Orogeny*. Geological Society of America, Boulder, Colorado, pp. 211–227.
- Vanderhaeghe, O., 2009. Migmatites, granites and orogeny: flow modes of partially-molten rocks and magmas associated with melt/solid segregation in orogenic belts. *Tectonophysics* 477, 119–134 doi:110.1016/j.tecto.2009.1006.1021.

- Vanderhaeghe, O., Kruckenberg, S.C., Gerbault, M., Martin, L., Duchêne, S., Deloule, S., 2018. Crustal-scale convection and diapiric upwelling of a partially molten T orogenic root (Naxos dome, Greece). *Tectonophysics* 746, 459–469. <https://doi.org/10.1016/j.tecto.2018.03.007>.
- Walcott, C.R., White, S.H., 1998. Constraints on the kinematics of post-orogenic extension imposed by stretching lineations in the Aegean region. *Tectonophysics* 298, 155–175.
- Wijbrans, J.R., McDougall, I., 1988. Metamorphic evolution of the Attic Cycladic Metamorphic Belt on Naxos (Cyclades, Greece) utilizing $^{40}\text{Ar}/^{39}\text{Ar}$ age spectrum measurements. *J. Metamorph. Geol.* 6, 571–594 doi:510.1111/j.1525-1314.1988.tb00441.x.